PERGAMON Computers and Mathematics with Applications 41 (2001) 783–811

An International Journal
computers & mathematics
with applications

www.elsevier.nl/locate/camwa

A Mathematical Model for the Study of Interstitial Fluid Movement Vis-a-Vis the Non-Newtonian Behaviour of Blood in a Constricted Artery

J. C. MISRA AND S. K. GHOSH*
Department of Mathematics
Indian Institute of Technology
Kharagpur 721302, India

(Received February 1999; accepted March 1999)

Abstract—A mathematical model is developed with an aim to study the transport of interstitial fluid in the wall of a constricted artery by taking into account the microrotation of the erythrocytes of blood. The movement of the interstitial fluid has been described by the Debye-Brinkman equation. Exact solutions are obtained for the displacement of the solid matrix of the porous interstitial space, the velocity of the interstitial fluid movement, and the pressure distribution in the constricted arterial segment, for large and small consolidation times. Expression for the wall shear stress is also obtained for the constricted segment of the artery. Theoretical estimates of the distributions of the axial velocity of blood in the stenosed zone, rotational velocity of the erythrocytes, wall shear stress, and wall displacement, as well as the pressure and velocity profiles for the interstitial fluid movement, have been presented in the form of graphs.

NOMENCLATURE

ϵ'	height of the stenosis	ν	Poisson's ratio
k	a constant	ν^*	$(1-2\nu)/(1-\nu)$
δ_{ij}	Kronecker delta	ω	angular frequency
E_{ij}	infinitesimal strain tensor	p_1	pressure in porous space
G, λ	stiffness constants	p_{ti}	$\frac{\partial p}{\partial x_i}$ the pressure gradient
h	thickness of the normal arterial wall	r	radial coordinate
i	$\sqrt{-1}$	a	characteristic radius of the artery
I_0, I_1	modified Bessel functions of the first kind	R^*	internal radius
		t	time
K_0, K_1	modified Bessel functions of the second kind	T_{ij}	composite stress of mixture
		τ	consolidation time
K_p	permeability of the matrix	τ_{ij}	contact stress
μ	viscosity of the interstitial fluid		

*Presently at Garbeta College, Garbeta, Midnapore, India.

This research was supported by CSIR Grant No. 95/81(244)/9-EMR-I.

0898-1221/01/$ - see front matter Typeset by AMS-TEX
PII: S0898-1221(00)00320-5

u_i	displacement vector	μ_r, μ_s	rotational and shear viscosity
v_{si}	solid velocity	ψ	stream function
V_i	total velocity	U_0	mean axial velocity at $r = 0$
w_i	filtration velocity	U_1	porous space solid displacement along radial direction
x	axial distance	w	porous space fluid displacement along radial direction
u, v	axial and radial velocity of blood	p_t	transmural pressure of blood
ν_θ	rotational velocity along θ direction		

1. INTRODUCTION

The deposit of cholesterol on the endothelium and proliferation of connective tissues in an arterial wall form plaques which grow inward and restrict the flow of blood through the lumen of the artery. Arterial diseases such as this have been quite widespread now-a-days, and hence, studies pertaining to their cause and development are receiving intensified attention of researchers from various disciplines. Different aspects of the problem are being investigated from different angles. In order to have a better understanding of the formation, growth, and development of stenosis, it is definitely essential that together with studies pertaining to flow characteristics of blood and the deformation and stress field generated in the wall, the movement of the interstitial fluid in the porous matrix of the arterial wall should be paid due attention. Although in the past there have been some extensive theoretical studies relating to blood flow, as well as wall deformations under normal and pathological conditions [1–11], the problem of fluid flow in the interstitial space of the arterial wall, as well as the associated problem of transport of nutrients from blood to the adjacent tissue medium through the pores in the walls of smaller blood vessels has received scant attention. Kenyon [12,13] made a theoretical analysis for the time-dependent filtration of fluids through the walls of soft porous tubes. Following [13], some attempt was made to study the interstitial fluid flow [14] by using Darcy's law to relate the said flow to the pore pressure. However, previous studies such as this suffer from the inherent deficiency that they do not account for the no-slip condition on the coarse fibers of the wall tissues. As pointed out by Ethier [15], the coarse fibers create velocity gradients within the fine material due to the fact that the no-slip condition must be satisfied on the surface of the coarse fibers. These coarse fibers also increase the superficial velocity through the fine material due to the effect of area obstruction, and also contribute to increasing the overall tortuosity of the mixed material. All these effects produced by the coarse fibers of the wall tissues have an important bearing on the reduction of the permeability of the wall tissues.

In order to take care of these obstructions, it is suggested that studies pertaining to the interstitial fluid movement in the porous matrix of the arterial wall be carried out by using the Debye-Brinkman equation (rather than Darcy's law) that bears the potential to account for the presence of the porous matrix by inclusion of a bulk stress term.

In the present paper, we make an attempt to develop a mathematical model for the study of the interstitial fluid movement in the fibrous medium of a stenosed arterial wall by using the Debye-Brinkman equation to describe the transmural flow. The solid phase of the porous matrix is considered to be elastic while the fluid phase is taken to be incompressible. Under the purview of the same model, simultaneously we pay full attention to the flow of blood in the lumen of the constricted artery, keeping in view the fact that the flow characteristics of blood contribute to the interstitial fluid flow and vice versa. Blood is treated as a non-Newtonian fluid in this analysis owing to the fact that surrounding the constriction shear rate of blood is low [16] and experimental observation that blood exhibits non-Newtonian behaviour in the low shear-rate region [17,18]. Taking cognizance of the observations made by Ariman *et al.* [19] and [20] that the erythrocytes of blood have a microrotation at low shear rates, in the mathematical model developed here, blood is considered as a micropolar fluid.

The available literature on the movement of interstitial fluid in arterial walls reveals that the large pressure gradients are mostly confined to narrow boundary layers and that in large arteries the consolidation time, that is the time taken by the boundary layer, or the fluid drainage front to extend over the full width of the arterial wall is usually very large. Keeping this in mind, in the present study, particular attention is paid to the case of large consolidation time, and the results are compared with those for the situation when the consolidation time is small.

The time-dependence of the pressure and the velocity of the fluid matrix, as well as that of the displacement of the solid matrix in the interstitial space has been paid due attention while analyzing the mathematical model. The study is carried out for constrictions formed in the pathological state of an artery formed by atherosclerotic plaques, as well as constrictions in a normal artery formed by some mechanical means. With an aim to illustrate the applicability of the mathematical model, the analytical solution of the model is applied to determine theoretical estimates of some quantities that describe the flow in the lumen of the artery, as well as various quantities depicting the deformation and flow characteristics of the interstitial space of the arterial wall, by using typical values of the system parameters.

2. MATHEMATICAL MODEL OF BLOOD FLOW IN THE STENOSED ARTERY

Let us consider an axially symmetric laminar pulsatile flow of blood through a cylindrical segment of an artery having a stenosis (Figure 1). The geometry of the stenosis is described mathematically as

$$R^*(x) = \begin{cases} a - \dfrac{\epsilon'}{2}\left(1 + \cos\dfrac{2\pi}{L}\left(x - d - \dfrac{L}{2}\right)\right), & d \le x \le d + L, \\ a, & \text{otherwise}, \end{cases} \tag{1}$$

where a is the characteristic radius of the artery, ϵ' the stenosis height, and L the length of the stenosis.

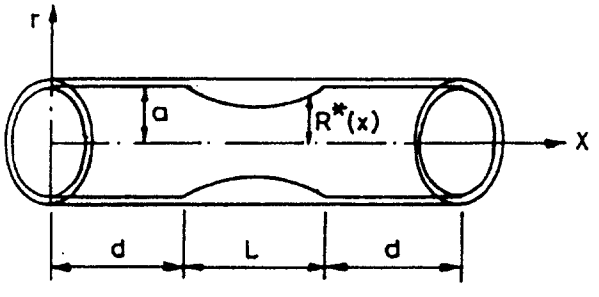

(a) Atherosclerotic constriction.

Let us consider the velocity components and pressure in the form

$$\begin{aligned} u &= u_r(r)e^{i(\omega t - k_1 x)}, \qquad v = v_x(r)e^{i(\omega t - k_1 x)}, \qquad p = p_{t1}(r)e^{i(\omega t - k_1 x)}, \\ \nu_\theta &= \nu_{\theta 1}(r)e^{i(\omega t - k_1 x)}, \qquad \Omega = \Omega_1(r)e^{i(\omega t - k_1 x)}. \end{aligned} \tag{2}$$

Existing literature shows that the micropolar approach is suitable to treat blood as a fluid suspension containing spherical nondeformable particles enabling one to describe the rotational motion of red blood cells through a dynamic kinematical variable (microrotational vector). In this approach, one is limited in not being able to account for the cell shape and the deformations it undergoes during shear flow. However, red cell deformability is not significant at low shear rates (the red cells rotate almost like rigid particles).

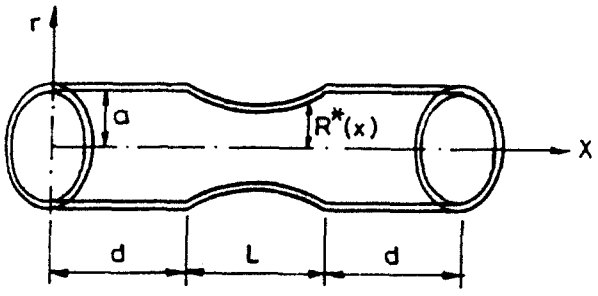

(b) Constriction by mechanical means.

Figure 1.

Application of the micropolar continuum theory to a general blood flow problem requires the determination of seven unknowns, viz. the pressure $p(X,t)$, the three components of $\vec{V}(X,t)$, and the three components of $\vec{\nu}(X,t)$.

The vectorial forms of these governing field equations are

$$(\lambda_s + 2\mu_s)\nabla\nabla\cdot\vec{V} - (\mu_s+\mu_r)\nabla\times\nabla\times\vec{V} + 2\mu_r(\nabla+\vec{\nu}) - \nabla p + \rho\vec{F} = \rho\left[\frac{\partial\vec{V}}{\partial t} - \vec{V}\times\left(\nabla\times\vec{V}\right) + \frac{1}{2}\nabla\left(\vec{V}^2\right)\right], \tag{3}$$

$$(\alpha+\beta+\gamma)\nabla\nabla\cdot\vec{\nu} - \gamma\nabla\times\nabla\times\vec{\nu} + 2\mu_r\nabla\times\vec{V} - 4\mu_r\vec{\nu} + \rho\vec{I} = \rho j\dot{\vec{\nu}}, \tag{4}$$

while the equation of continuity is

$$\frac{\partial\rho}{\partial t} + \nabla\cdot\left(\rho\vec{V}\right) = 0, \tag{5}$$

where the superimposed dot on the right-hand side of equation (4) denotes material differentiation; $\vec{V}$ is velocity, $\vec{\nu}$ the microrotation, $\vec{F}$ the body force, $\vec{I}$ the body couple vector, j (constant) gyration tensor parameter, ρ the density, and p the pressure, while λ_s, μ_r, μ_s, α, β, γ are different material constants.

Considering the flow to be axisymmetric, we take $u_\theta = 0$ and $\nu_r = 0 = \nu_x$. The analysis will be carried out by taking the haematocrits to be neutrally buoyant and assuming that there are no body forces or couples. With all these considerations, equations (3)–(5) in the cylindrical coordinate system reduce to

$$-(\mu_r+\mu_s)\frac{\partial\Omega}{\partial x} - 2\mu_r\frac{\partial\nu_\theta}{\partial x} - \frac{\partial p_t}{\partial r} = \rho\left(\frac{\partial v}{\partial t} + u\frac{\partial v}{\partial x} + v\frac{\partial v}{\partial r}\right), \tag{6}$$

$$(\mu_s+\mu_r)\left(\frac{\partial\Omega}{\partial r} + \frac{\Omega}{r}\right) + 2\mu_r\left(\frac{\partial\nu_\theta}{\partial r} + \frac{\nu_\theta}{r}\right) - \frac{\partial p_t}{\partial x} = \rho\left(\frac{\partial u}{\partial t} + u\frac{\partial u}{\partial x} + v\frac{\partial u}{\partial r}\right), \tag{7}$$

$$\gamma\nabla^2\nu_\theta - 2\mu_r\Omega - 4\mu_r\nu_\theta = \rho j\frac{\partial\nu_\theta}{\partial t}, \tag{8}$$

where

$$\nabla^2 = \left(\frac{\partial^2}{\partial r^2} + \frac{1}{r}\frac{\partial}{\partial r} - \frac{1}{r^2} + \frac{\partial^2}{\partial x^2}\right), \qquad \Omega = \left(\frac{\partial u}{\partial r} - \frac{\partial v}{\partial x}\right).$$

On account of no-slip on the endothelium, we write

$$u = 0, \qquad r = R^*(x). \tag{9}$$

Further, since the axial velocity is maximum ($= U_0$, say) on the centerline of the artery, we have

$$u = U_0, \qquad r = 0. \tag{10}$$

The total flux can then be written as

$$\int_0^{R^*(x)} \int_0^{2\pi} ru\, dr\, d\theta = 2\pi\psi_0, \tag{11}$$

ψ_0 being the value of the stream function at the wall.

3. MODEL OF THE WATER FLUX IN THE ARTERIAL WALL

Here, the wall of the artery will be considered to be composed of a mixture of a porous incompressible elastic solid matrix and an incompressible liquid [12]. Then, the equation that governs the equilibrium of the wall tissues can be taken to be

$$T_{ij,j} = \tau_{ij,j} - p_{1,j} = 0, \tag{12}$$

$\tau_{ij,j}$ being the stress tensor that depends on the bulk deformation of the matrix, called the 'contact stress' in the sequel, and p_1 the pressure exerted by the interstitial fluid. The following equation is taken to describe the flow of the interstitial fluid:

$$p_{1,i} = \mu\left(\beta w_{i,ii} - \frac{1}{K_p} w_i\right). \tag{13}$$

When $\beta = 0$, the equation reduces to Darcy's law, while for $\beta = 1$, equation (13) gives rise to the Debye-Brinkman equation that was used by Wang *et al.* [21]; w_i is the filtration velocity of the interstitial fluid relative to the matrix, and μ stands for the viscosity of the fluid in the porous space.

The volume flux conservation equation is given by

$$V_{i,i} = 0, \tag{14}$$

where $V_i = w_i + v_{si}$ and v_{si} is the solid velocity (averaged macroscopically). The linear approximation for the relation between the contact stress τ_{ij} and the infinitesimal strain $E_{ij} = (1/2)(U_{i,j} + U_{j,i})$ is given by

$$\tau_{ij} = \lambda E_{kk}\delta_{ij} + 2GE_{ij}. \tag{15}$$

We consider a cylindrical polar coordinate system with r as the radial distance and x the axial distance. The endothelial layer and the adventitia are, respectively, given by $r = R^*(x)$ and $r = R^*(x) + h$, h being the thickness of the arterial wall. Equations (12)–(15) can be written as

$$\frac{\partial p_1}{\partial r} = \mu\beta\left(\frac{\partial^2 w}{\partial r^2} + \frac{1}{r}\frac{\partial w}{\partial r} - \frac{w}{r^2} + \frac{\partial^2 w}{\partial x^2}\right) - \frac{\mu}{K_p} w, \tag{16}$$

$$(\lambda + 2G)\left(\frac{\partial^2 U_1}{\partial r^2} + \frac{1}{r}\frac{\partial U_1}{\partial r} - \frac{U_1}{r^2}\right) + G\frac{\partial^2 U_1}{\partial x^2} = \frac{\partial p_1}{\partial r}. \tag{17}$$

The continuity equation for the bulk material is

$$\frac{\partial}{\partial r}\left(\frac{\partial U_1}{\partial t} + w\right) + \frac{1}{r}\left(\frac{\partial U_1}{\partial t} + w\right) = 0. \tag{18}$$

Because of the continuity of the radial velocity of the wall tissue and the blood, and also of the normal stress along the endothelium, we have

$$v = \frac{\partial U_1}{\partial t} + w, \qquad r = R^*(x), \tag{19}$$

$$-p_t + 2(\mu_s + \mu_r)\frac{\partial v}{\partial r} = (\lambda + 2G)\frac{\partial U_1}{\partial r} + \lambda\frac{U_1}{r}, \qquad r = R^*(x). \tag{20}$$

At the endothelium, the interstitial fluid pressure is equal to the transmural pressure, while the pressure on the adventitia is zero. These conditions may be described mathematically as

$$p_1 = p_t, \qquad r = R^*(x), \tag{21}$$

$$p_1 = 0, \qquad r = R^*(x) + h. \tag{22}$$

Considering the adventitia to be traction-free, we write

$$(\lambda + 2G)\frac{\partial U_1}{\partial r} + \lambda\frac{U_1}{r} = 0, \qquad r = R^*(x) + h. \tag{23}$$

4. SOLUTION FOR THE HEMODYNAMIC FLOW

Implicit in the use of the linearized form of Navier-Stokes equations is the assumption that the convective acceleration terms can be ignored with respect to the linear terms. Thus, eliminating p_t from the linearized version of (6),(7) and then by using (8), we obtain

$$\frac{(\mu_s + \mu_r)}{\rho}\nabla^2\Omega_1 + \frac{2\mu_r^2}{\rho\gamma}\Omega_1 + \frac{2\mu_r}{\gamma}\left(\frac{4\mu_r}{\rho} + i\omega j\right)\nu_{\theta 1} = i\omega\Omega_1. \tag{24}$$

Operating both sides of this equation by ∇^2, we find

$$\frac{2\mu_r}{\gamma}\left(\frac{4\mu_r}{\rho} + i\omega j\right)\nabla^2\nu_{\theta 1} = -\frac{(\mu_s + \mu_r)}{\rho}\nabla^4\Omega_1 + \left(i\omega - \frac{2\mu_r^2}{\rho\gamma}\right)\nabla^2\Omega_1. \tag{25}$$

Introducing nondimensional variables

$$\tilde{r} = \frac{r}{a}, \qquad \tilde{x} = \frac{x}{a}, \qquad \tilde{\Omega}_1 = \frac{\Omega_1 a^3}{\psi_0}, \qquad \tilde{p}_t = \frac{p_t a^3}{\psi_0 \mu}, \qquad \text{and} \qquad \tilde{\nu}_\theta = \frac{\nu_\theta a^3}{\psi_0},$$

and substituting (24) and (25) into equation (8) and writing the nondimensional quantities without, we get

$$\left(A_n\nabla^4 + B_n\nabla^2 + C_n\right)\Omega_1 = 0; \tag{26}$$

the expressions for A_n, B_n, and C_n are given by

$$A_n = (\mu_r + \mu_s)\gamma,$$

$$B_n = -\left[(\mu_s + \mu_r)\left(4\mu_r a^2 + ij\alpha^2(\mu_s + \mu_r)\right) + \left(i\gamma\alpha^2(\mu_s + \mu_r) - 4\mu_r^2 a^2\right)\right],$$

$$C_n = \left[\alpha^2(\mu_s + \mu_r)\left(4\mu_r^2 a^2 + ij\alpha^2(\mu_s + \mu_r)\right)\right], \qquad \alpha^2 = \frac{\omega\rho a^2}{(\mu_s + \mu_r)}.$$

The biharmonic equation (26) can be rewritten in the form

$$\left(\nabla^2 - A_{11}'^2\right)\left(\nabla^2 - A_{12}'^2\right)\Omega_1 = 0, \tag{27}$$

where

$$A_{11}'^2 = \frac{-B_n + \sqrt{B_n^2 - 4A_nC_n}}{2A_n}, \qquad A_{12}'^2 = \frac{-B_n - \sqrt{B_n^2 - 4A_nC_n}}{2A_n}.$$

The solution of (27) is obtained as

$$\Omega_1 = \left(CI_1(A_{12}r) - \frac{M_1 I_1(A_{11}r)}{A_{11}^2 - A_{12}^2}\right), \tag{28}$$

where $A_{11}^2 = k^2 + A_{11}'^2$, $A_{12}^2 = k^2 + A_{12}'^2$, $k = k_1 a$.

Expressing Ω_1 in terms of the stream function ψ and using (28), we have

$$\left(\frac{1}{r}\frac{\partial^2}{\partial r^2} - \frac{1}{r^2}\frac{\partial}{\partial r} + \frac{1}{r}\frac{\partial^2}{\partial x^2}\right)\psi = \left(CI_1(A_{12}r) - \frac{M_1 I_1(A_{11}r)}{A_{11}^2 - A_{12}^2}\right). \tag{29}$$

The solution of this equation is given by

$$\psi = \left(iA_T' r I_1(kr) - \frac{CrI_1(A_{12}r)}{A_{12}^2 - k^2} + \frac{M_1 r I_1(A_{11}r)}{(A_{11}^2 - A_{12}^2)(A_{11}^2 - k^2)}\right), \tag{30}$$

where A_T', C, and M_1 are arbitrary constants. Using the boundary conditions (9)–(11) in their nondimensional forms, we have calculated them; their derived expressions are included in Appendix I.

Putting (28) into the linearized version of (8), we get

$$\nu_{\theta 1} = C' I_1(B_{11}r) - \frac{2a^2}{\gamma}\left(\frac{CI_1(A_{12}r)}{(A_{12}^2 - B_{11}^2)} - \frac{M_1 I_1(A_{11}r)}{(A_{11}^2 - A_{12}^2)(A_{11}^2 - B_{11}^2)}\right), \tag{31}$$

where

$$B_{11}^2 = \frac{\rho a^2}{\gamma}\left(\frac{4\mu_r}{\rho} + ij\omega\right) + k^2.$$

While C and M_1 are already known, C' is determined by using the following condition for the cell-rotational velocity on the wall of the stenosed arterial segment:

$$\frac{1}{r}\frac{d}{dr}(r\nu_{\theta 1}) = 0, \qquad r = R(x). \tag{32}$$

In order to calculate the transmural pressure, we substitute (30) and (31) into the linearized version of equation (6) (the expression for v calculated by using the expression for the stream function has also been used). Integrating the resulting equation with respect to r and using (2), we obtain

$$\begin{aligned} p_t = \frac{1}{\mu}\Bigg[&\{-\alpha^2(\mu_s + \mu_r)iA_T' I_0(kr)\} + C\left\{\frac{k\alpha^2(\mu_s + \mu_r)I_0(A_{12}r)}{A_{12}(A_{12}^2 - k^2)} + k(\mu_s + \mu_r)i\frac{I_0(A_{12}r)}{A_{12}}\right. \\ &\left. - \frac{4i\mu_r^2 k}{\gamma A_{12}}\frac{I_0(A_{12}r)}{(A_{12}^2 - B_{11}^2)}\right\} + \frac{M_1}{A_{11}(A_{11}^2 - A_{12}^2)}\left\{-\frac{\alpha^2(\mu_s + \mu_r)kI_0(A_{11}r)}{(A_{11}^2 - k^2)}\right. \\ &\left. - i(\mu_r + \mu_s)kI_0(A_{11}r) + \frac{4i\mu_r^2 k}{\gamma}\frac{I_0(A_{11}r)}{(A_{11}^2 - B_{11}^2)}\right\} + C'\frac{2ik\mu_r I_0(B_{11})}{B_{11}r} + K\Bigg] e^{i(\omega t - kx)}, \end{aligned} \tag{33}$$

where K is an arbitrary constant.

The stress tensor for the micropolar fluid is given by Ariman *et al.* [22],

$$\sigma_{ij} = (-\pi + \lambda v_{r,r})\delta_{ij} + \mu_r(v_{i,j} + v_{j,i}) + \mu_s(v_{j,i} - e_{ijr}\nu_r). \tag{34}$$

The wall shear stress can then be obtained by using the equation

$$\tau_w = \frac{\left\{\sigma_{xr}\left[1 - \left(\frac{dR}{dx}\right)^2\right] + (\sigma_{rr} - \sigma_{xx})\frac{dR}{dx}\right\}}{\left\{1 + \left(\frac{dR}{dx}\right)^2\right\}}, \tag{35}$$

where the expressions for σ_{xr} and $\sigma_{rr} - \sigma_{xx}$ as calculated from (30) are

$$\sigma_{xr} = \left[\left\{\frac{(\mu_r + \mu_s)}{R^2}\left(k^2 i A_T' I_1(kR) - CA_{12}^2 \frac{I_1(A_{12}R)}{(A_{12}^2 - k^2)} + M_1 \frac{A_{11}^2 I_1(A_{11}R)}{(A_{11}^2 - A_{12}^2)(A_{11}^2 - k^2)}\right)\right\}\right.$$
$$+ \mu_r \left\{C' I_1(B_{11}R) + \frac{2\mu_r}{\gamma}\left(-C\frac{I_1(A_{12}R)}{(A_{12}^2 - B_{11}^2)} + M_1 \frac{I_1(A_{11}R)}{(A_{11}^2 - A_{12}^2)(A_{11}^2 - B_{11}^2)}\right)\right\}$$
$$+ \mu_r k^2 \left\{i A_T' I_1(kR) - C\frac{I_1(A_{12}R)}{(A_{12}^2 - k^2)}\right.$$
$$\left.\left. + M_1 \frac{I_1(A_{11}R)}{(A_{11}^2 - A_{12}^2)(A_{11} - k^2)}\right\}\right] e^{i(\omega t - kx)}, \tag{36}$$

$$\sigma_{rr} - \sigma_{xx} = \frac{ik(\mu_r + \mu_s)}{R}\left[i A_T' I_1(kR) - 2CA_{12}R\frac{I_0(A_{12}R)}{(A_{12}^2 - k^2)}\right.$$
$$+ 2M_1 A_{11} R \frac{I_0(A_{11}R)}{(A_{11}^2 - A_{12}^2)(A_{11}^2 - k^2)} - 2A_T' kR I_0(kR) + C\frac{I_1(A_{12}R)}{(A_{12}^2 - k^2)}$$
$$\left. - M_1 \frac{I_1(A_{11}R)}{(A_{11}^2 - A_{12}^2)(A_{11}^2 - k^2)}\right] e^{i(\omega t - kx)}. \tag{37}$$

5. SOLUTION FOR THE WALL MEDIUM

We consider the displacement components and the pressure to be given by

$$w = \bar{w} e^{i(\omega t - k_1 x)}, \qquad U_1 = \bar{U}_1' e^{i(\omega t - k_1 x)}, \qquad p_1 = \bar{p}_1 e^{i(\omega t - k_1 x)}. \tag{38}$$

Substituting (38) into equations (16)–(18) and applying the boundary conditions (19)–(23), we obtain the following equations in terms of the nondimensional variables introduced earlier:

$$\bar{w} = \frac{\bar{A}}{r} - \bar{U}_1 i\omega, \tag{39}$$

$$\eta^2 \frac{d\bar{U}_1^2}{d\eta^2} + \eta \frac{d\bar{U}_1}{d\eta} - \left(1 + H_1^2 \eta^2\right)\bar{U}_1 = \frac{A'}{\eta} H_2, \tag{40}$$

$$\frac{\partial \bar{p}_1}{\partial \eta} = \frac{H_4}{H_3}\bar{U}_1 - \frac{A' H_5}{\eta H_3}. \tag{41}$$

Solutions in nondimensionalized form are given by

$$\bar{U}_1 = A I_1(H_1\eta) + B K_1(H_1\eta) + \frac{A' H_2}{\eta}, \tag{42}$$

$$\bar{p}_1 = \frac{H_4}{H_3 H_1}\{A I_0(H_1\eta) + B K_0(H_1\eta)\} + \frac{A'}{H_3}(H_2 H_4 - H_5)\log(\eta) + E, \tag{43}$$

where

$$\eta = \frac{r}{\delta}, \qquad \delta^2 = \left\{\frac{(\lambda + 2G) + \mu i\beta\omega}{i\omega(\mu/K_p)}\right\},$$
$$H_1^2 = \left\{\frac{Gk^2 + k^2\mu\beta i\omega}{i\omega(\mu/K_p)} + 1\right\} a^2, \qquad H_2^2 = \left[\frac{\beta K^2 \mu}{\mu/K_p} + 1\right],$$
$$A' = \frac{\bar{A}}{\delta\omega i}, \qquad \bar{U}_1 = \frac{\bar{U}_1'}{a},$$
$$H_5 = \left(1 + k^2\beta K_p - \frac{H_2 \beta K_p}{\delta}\right), \qquad H_3 = \left[\frac{(\delta^2 - \beta K_p)}{(\lambda + 2G)}\frac{\psi\mu}{\delta a^3}\right],$$

$$H_4 = \left\{a^2\left(\beta k^2 K_p + 1\right) - \frac{\beta K_p H_1^2}{\delta^2}\right\}, \qquad R_1(x) = R(x) + \frac{h}{a}.$$

A, B, A', and E are given in Appendix I.

The analytical expressions presented above are functions of $\eta\ (= r/\delta)$ which is complex since δ is complex. It is found that the characteristic consolidation time is proportional to the hydraulic resistance (μ/K_p) to the flow of the interstitial fluid and inversely proportional to the compressive stiffness $(\lambda + 2G)$ of the wall tissues, when $\omega\tau = h^2(\omega(\mu/K_p) + \mu i\omega\beta)/(\lambda + 2G)$ is large or when it is small. Since both of these cases are of particular interest, the remaining part of our study will be confined to these limiting cases only. The effect of the large and small consolidation time on the displacement of the solid matrix and the radial flow of the interstitial fluid will be investigated by using the following asymptotic expressions that have been derived by considering the asymptotic expansions of Bessel functions of large/small arguments [23].

For large consolidation time,

$$\begin{aligned} U_1 = \Bigg[&\left\{A_1 I_{r1} - A_2 I_{r2} + B_1 K_{r1} - B_2 K_{r2} + \frac{H_2 h\left(A_1' h_{11} - A_2' h_{12}\right)}{r\left(h_{11}^2 + h_{12}^2\right)}\right\}\cos(\omega t - kx) \\ &- \left\{A_1 I_{r2} + A_2 I_{r1} + B_1 K_{r2} + B_2 K_{r1} + \frac{H_2 h(A_1' h_{12} + A_2' h_{11})}{r(h_{11}^2 + h_{12}^2)}\right\}\sin(\omega t - kx)\Bigg], \end{aligned} \tag{44}$$

$$\begin{aligned} p_1 = \Bigg\{\Bigg[&H_c\left[A_1 I_{r01} - A_2 I_{r02} + B_1 K_{r01} - B_2 K_{r02}\right] \\ &- H_d\left[A_1 I_{r02} + I_{r01} A_2 + B_1 K_{r02} + B_2 K_{r01}\right] \\ &+ \left(A_1' h_{p31} - A_2' h_{p32}\right)\log Y - \tan^{-1}\frac{h_{12}}{h_{11}}\left(A_2' h_{p31} + A_1' h_{p32}\right) + E_1\Bigg]\cos(\omega t - kx) \\ &- \Bigg[H_c\left[A_1 I_{r02} + A_2 I_{r01} + B_1 K_{r02} + B_2 K_{r01}\right] \\ &+ H_d\left[A_1 I_{r01} - I_{r02} A_2 + B_1 K_{r01} - B_2 K_{r02}\right] + \left(A_1' h_{p31} - A_2' h_{p32}\right)\tan^{-1}\frac{h_{12}}{h_{11}} \\ &+ \log Y\left(A_2' h_{p31} + A_1' h_{p32}\right) + E_2\Bigg]\sin(\omega t - kx)\Bigg\}. \end{aligned} \tag{45}$$

For small consolidation time,

$$\begin{aligned} U_1 = \Bigg[&\left\{A_{1s} I_{sr1} - A_{2s} I_{sr2} + B_{1s} K_{sr1} - B_{2s} K_{sr2} + \frac{H_2 h\left(A_{1s}' h_{11} - A_{2s}' h_{12}\right)}{r\left(h_{11}^2 + h_{12}^2\right)}\right\}\cos(\omega t - kx) \\ &- \left\{A_{1s} I_{sr2} + A_{2s} I_{sr1} + B_{1s} K_{sr2} + B_{2s} K_{sr1} + \frac{H_2 h\left(A_{1s}' h_{12} + A_{2s}' h_{11}\right)}{r\left(h_{11}^2 + h_{12}^2\right)}\right\}\sin(\omega t - kx)\Bigg], \end{aligned} \tag{46}$$

$$\begin{aligned} p_1 = \Bigg\{\Bigg[&H_c[A_{1s} I_{sr01} - A_{2s} I_{sr02} + B_{1s} k_{sr01} - B_{2s} K_{sr02}] \\ &- H_d[A_{1s} I_{sr02} + I_{sr01} A_{2s} + B_{1s} K_{sr02} + B_{2s} K_{sr01}] \\ &+ \left(A_{1s}' h_{p31} - A_{2s}' h_{p32}\right)\log Y - \tan^{-1}\frac{h_{12}}{h_{11}}\left(A_{2s}' h_{p31} + A_{1s}' h_{p32}\right) + E_{1s}\Bigg]\cos(\omega t - kx) \\ &- \Bigg[H_c[A_{1s} I_{sr02} + A_{2s} I_{sr01} + B_{1s} K_{sr02} + B_{2s} K_{sr01}] \\ &+ H_d[A_{1s} I_{sr01} - I_{sr02} A_{2s} + B_{1s} K_{sr01} - B_{2s} K_{sr02}] \\ &+ \left(A_{1s}' h_{p31} - A_{2s}' h_{p32}\right)\tan^{-1}\frac{h_{12}}{h_{11}} + \log Y\left(A_{2s}' h_{p31} + A_{1s}' h_{p32}\right) + E_{2s}\Bigg]\sin(\omega t - kx)\Bigg\}. \end{aligned} \tag{47}$$

The expressions for $\bar{U}_1$ and p_1 have been included in Appendices II and III, respectively. In both cases, the interstitial velocity w of the flow in the radial direction can be obtained by using (39).

6. RESULTS AND DISCUSSIONS

The primary objective of this investigation has been to study the flow of the interstitial fluid and the displacement of the solid matrix in the porous wall of a constricted arterial segment.

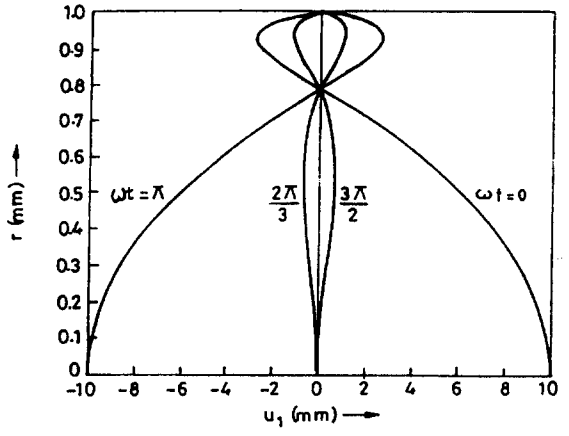

(a)

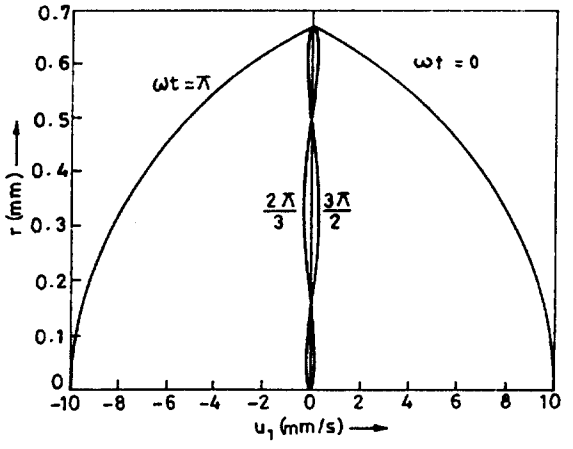

(b)

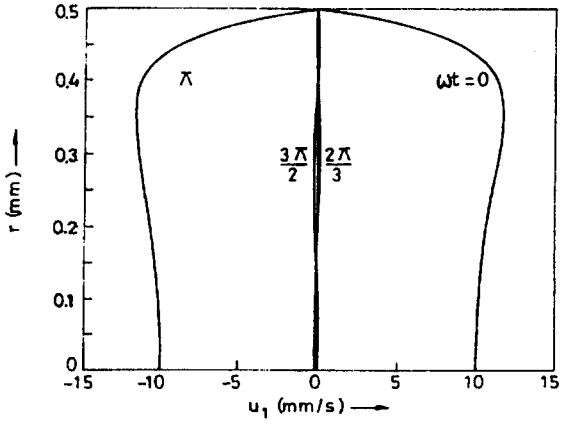

(c)

Figure 2. Axial velocity distribution of blood in the stenosed zone. At the axial positions (a) $x = 0.0$ mm, (b) 3.0 mm, and (c) 5.0 mm, the value for μ_r considered is 0.00018 kg m^{-1}sec^{-1}, and the values of other parameters are as given in the results and discussion section. At different instants of time, distribution of the axial velocity has been shown by different graphs. The results show that the axial velocity distributions are the same irrespective of whether the constriction has been formed due to atherosclerosis or some mechanical reason.

It is found that there exists a significant difference between the magnitudes of the flow velocity of blood, and the displacement in the solid matrix in the constricted artery is much different from the corresponding quantities in the case of a normal artery. The flow of blood has been considered to be pulsatile. In order to include the effect of microrotation of red cells, blood has been treated as a micropolar fluid. For the flow of blood, it has been assumed that the wave length is much larger than the axial velocity. The wall tissues are considered to be homogeneous, and the quantitative analysis is performed by taking average values of the different physical constants.

The computational work has been based upon the following experimental data available in the literature for canine femoral artery. $a = 1.0\,\text{mm}$, $U = 10.0\,\text{mm/sec}$, $\rho = 1.056 \times 10^3\,\text{kg/m}^3$, $G = 10^6\,\text{N/m}^2$, $\lambda = 4999 \times 10^6\,\text{N/m}^2$, $\nu = 0.5$ [1], $K_p/\mu = 5 \times 10^{-14}\,\text{m}^4/\text{N sec}$ [21], $h = 2 \times 10^{-4}\,\text{m}$ [14], $\gamma = 12 \times 10^{-17}\,\text{kg m/sec}$, $\mu_s = 0.00123\,\text{kg/m sec}$, $\mu_r = 0.00098\,\text{kg/m sec}$ (40% hematocrit [19]), $L = 10.0\,\text{mm}$, $\omega = 5.0\,\text{sec}^{-1}$, $K_p = 10^{-18}\,\text{m}^2$, and $j = 11.21 \times 10^{-9}\,\text{m}^2$.

Figure 2 gives the velocity profile of blood for the arterial segment under consideration. From Figure 2a which presents the results for $x = 0.0$, we observe that in the region where there is no stenosis, at any given instant of time, backflow occurs only in the vicinity of the wall. This possibly owes its origin to the fact that the microrotation of the cells is maximum in the region adjacent to the wall. Outside the stenotic region and also in some portion of the stenosed region, the magnitude of the axial velocity ($\omega t = 0, \pi$) attains its maximum value on the axis of the artery (cf. Figures 2a and 2b), except in the region where the height of the stenosis is maximum (cf. Figure 2c). We also observe that the flow disorder in the stenosed area is such that at any given instant of time, the flow takes place mostly either in the forward direction or in the backward direction throughout the cross-section of the stenosed portion of the arterial segment. Figure 3 shows that the rotational viscosity affects the cell rotational velocity only in the vicinity of the wall of the stenosed artery.

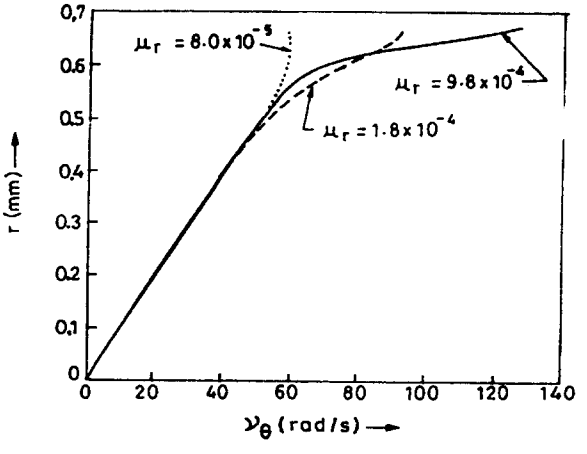

Figure 3. Distribution of rotational velocity of the erythrocytes. At the axial distance $x = 3.0\,\text{mm}$ of the stenosed zone at the time instant $\omega t = 0$, the three curves correspond to different values of μ_r. Here also the results are found to be independent of the cause of the constriction. These figures have been plotted by considering the value of the ratio ϵ to be 0.5.

The distribution of wall shear stress at different instants of time has been presented in Figure 4. A comparison between the results of Figures 4a and 4b reveals that the magnitude of the shear stress is significantly changed even due to small variation in the rotational viscosity of blood, although the points at which the maximum value is attained remain the same. These figures indicate that the shear stress diminishes with an increase in rotational velocity of the erythrocytes. This may be attributed to the fact that the axial velocity decreases as the rotational velocity increases.

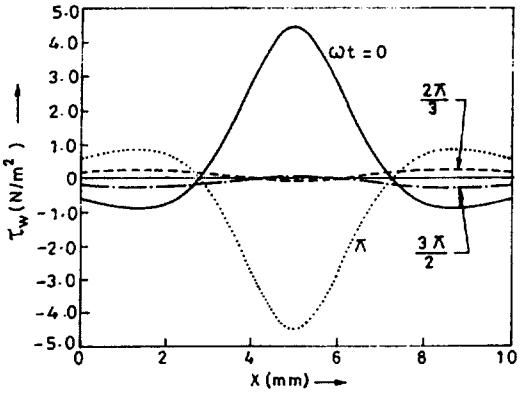

(a) $\mu_r = 9.8 \times 10^{-4}$ kg/m sec.

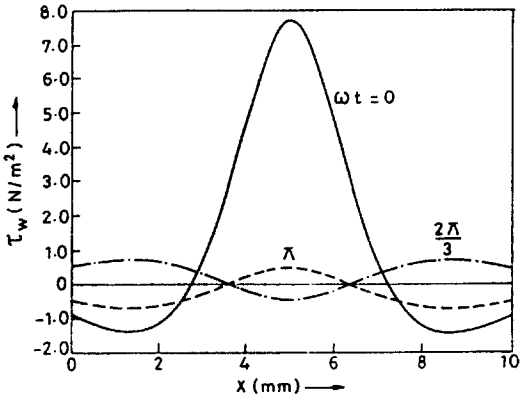

(b) 2.8×10^{-4} kg/m sec.

Figure 4. Wall shear stress at different axial stations and at different instants of time. The parameters used here are $\epsilon = 0.5$, $\gamma = 12 \times 10^{-13}$ kg m/sec.

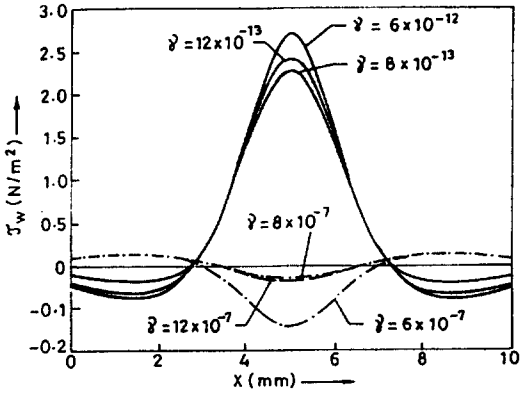

Figure 5. These curves present a comparison of wall shear stresses at two different instants, $\omega t = 0$ and $\omega t = 2\pi/3$, denoted by solid and dashed-dotted lines, respectively. At each instant of time, graphs have been plotted for three different values of the microrotational gradient parameter γ. Variations of the wall shear stress with axial distance reveal that the magnitude of the shear stress is maximum when the stenosis height is maximum. The values of the parameters considered are $\epsilon = 0.5$, $\mu_r = 9.8 \times 10^{-4}$ kg/m sec.

Figure 5 gives the shear stress distributions for different values of the microrotational gradient coefficient γ. It is noted that as γ increases, the magnitude of the shear stress increases. It is

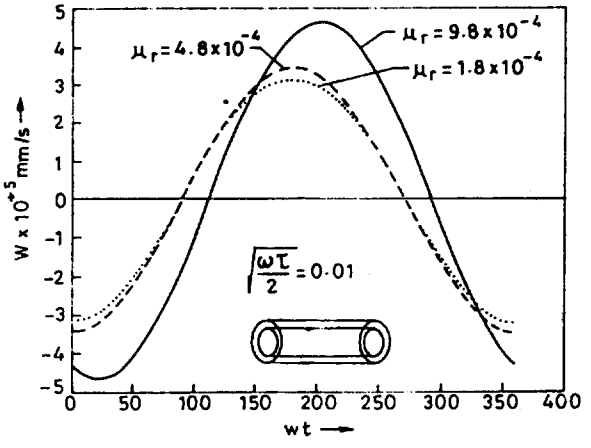

(a)

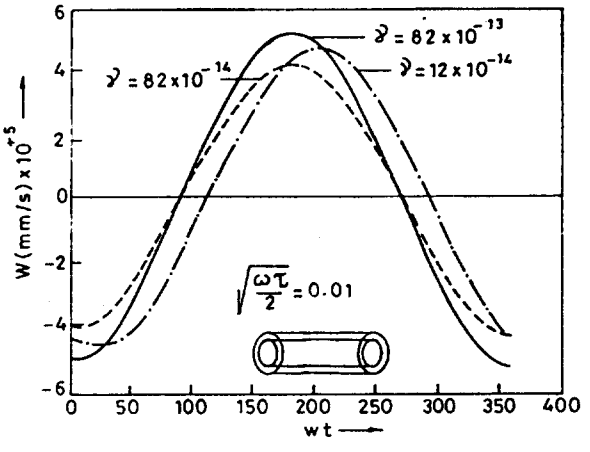

(b)

Figure 6. Variation of radial velocity in the interstitial space with time (when the consolidation time is small). This variation is considered in the nonstenotic situation. In Figure 6a, graphs have been plotted for different values of μ_r by taking $\gamma = 12 \times 10^{-13}$ kg m/sec, while graphs of Figure 6b are drawn for different values of γ, taking $\mu_r = 9.8 \times 10^{-4}$ kg/m sec. The results presented here correspond to an axial distance $x = 5$ mm.

possible to have some important ideas regarding the movement of the interstitial fluid in the porous wall tissue medium from Figure 6a. The results presented in this figure give us an insight of the variation of the interstitial fluid velocity in the radial direction due to change in the rotational viscosity of blood. The results presented in this figure have been computed for small consolidation time, that is, by assuming that the time required for the fluid drainage front to extend over the entire width of the arterial wall is small. It may be noted that the interstitial fluid velocity is enhanced due to an increase in the rotational viscosity of blood. This implies that the interstitial fluid movement is dependent upon the magnitude of the rotational viscosity of blood (μ_r). Figure 6b gives us similar ideas for the dependence of the movement of the interstitial fluid on the value of the other material constant γ (microrotational gradient coefficient) connected with cell rotation.

The computational results for the solid matrix of the arterial wall for a normal artery (in the absence of atherosclerotic plaques) have been presented in Figure 7. For the sake of comparison, the results reported by Jayaraman [14], who considered Darcy's law for the motion of the interstitial fluid, have been included in the same figure.

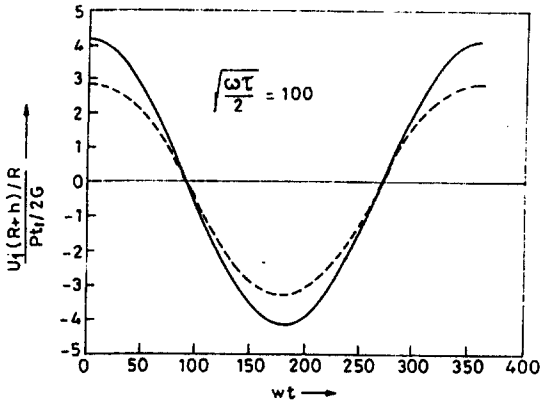

Figure 7. Variation of the arterial wall displacement with time in the absence of stenosis. The solid line gives the theoretical estimate computed with the consideration of Debye-Brinkman model for the interstitial flow, while the dashed line gives corresponding results of Jayaraman [14] calculated by using Darcy's law. A comparison between these two graphs reveals that the velocity gradients generated by the coarse fibers of the arterial wall bear the potential to enhance the wall displacement.

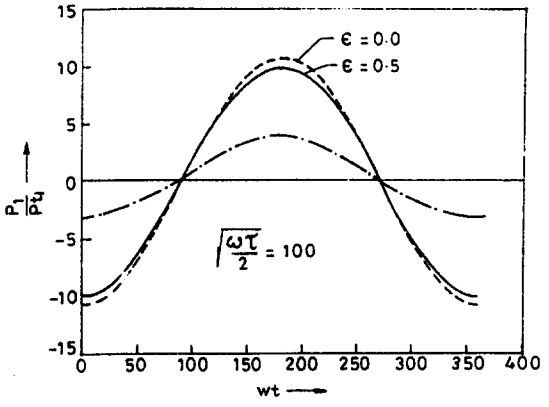

Figure 8. Time variation of pressure in the interstitial space for large consolidation time at a radial distance of 1.08 mm. The solid curve gives the said variation for a stenosed segment of an artery when $\epsilon = 0.5$, while the dotted curve gives the same for an arterial segment under identical conditions in the absence of stenosis in the context of present study; the dash-and-dot curve represents similar variation calculated under the purview of Darcy's law. The graphs indicate that for a mild stenosis such as the one considered in the present investigation, although the nature of time variation of pressure in the interstitial space in an arterial segment having a constriction created by some mechanical means is similar to that for a normal segment, a reduction in the magnitude of the pressure occurs particularly in the vicinity of the maximum height of the stenosis. Moreover, the velocity gradient created by the coarse fibers of the wall tissue enhances the magnitude of the interstitial pressure by an appreciable amount.

Figure 8 gives the variation of pressure in the interstitial space with time in the stenosed arterial segment, as well as for a normal artery. The results for the pressure variation for the normal artery are compared with the corresponding results by Jayaraman [14], who carried out a similar study by considering Darcy's law for the flow in the interstitial space. A comparison of our results for the stenosed artery with the corresponding results computed by us for the normal artery reveals that the instants of time at which the pressure attains its maximum are not affected by the presence of mild stenosis considered in the present investigation. We have taken into account in the present study the viscous force that is required to satisfy the no-slip boundary condition on the surface of the smooth muscle cells. A comparison of our results with those reported in [14] asserts that while this force has an appreciable influence on the variation

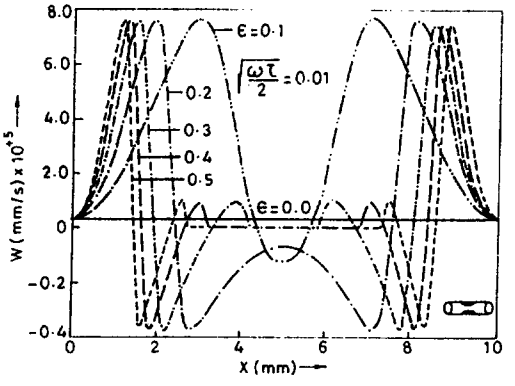

(a)

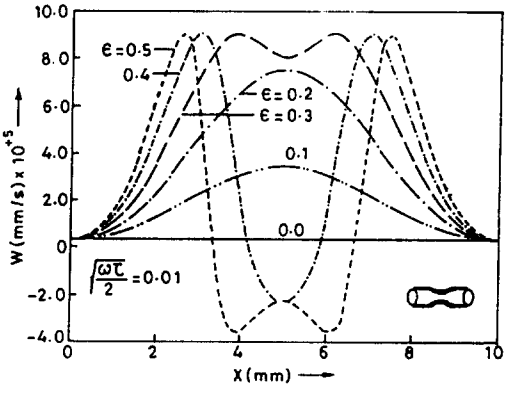

(b)

Figure 9. Variation of the radial velocity of the interstitial fluid in the adventitial layer at the point 0.02 mm below the outer surface of the artery along the axis of the artery for different constriction heights where the consolidation time is small: (a) when there is an atherosclerotic plaque formation, (b) when there is a constriction created by mechanical means. Configurations of both the cases are given in the corresponding figures. The instant of time for which computation has been carried out is given by $\omega t = \pi$.

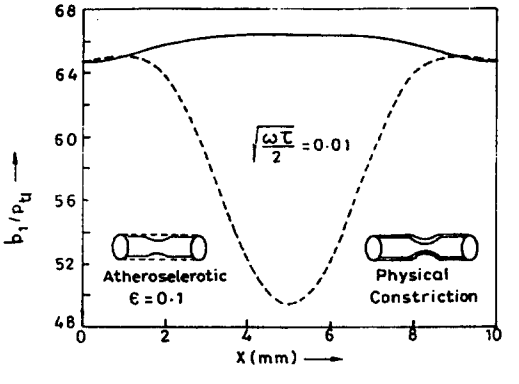

Figure 10. Variation of the pressure ratio p_1/p_{t1} in the axial direction, p_1 being the interstitial fluid pressure and p_{t1} the transmural pressure at the inner wall of the constricted segment of the artery in the intima, 0.02 mm above the endothelium. The solid line gives the variation when the constriction is created by some mechanical means, while the dotted line gives the same when the constriction owes its origin to the formation of an atherosclerotic plaque. Here, $\omega t = \pi$ and the consolidation time is considered to be small. The figures reveal that the said variation is strongly dependent on the manner in which the constriction has been formed.

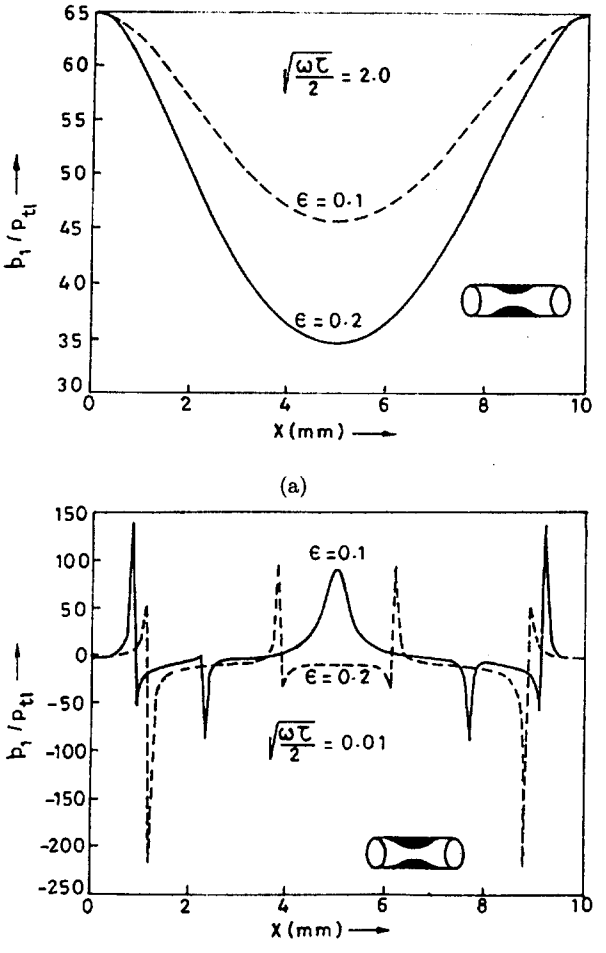

Figure 11. (a) and (b) represent the variation of the pressure ratio for large and small consolidation times, respectively. The results are presented for two different stenotic heights of an atherosclerotic constriction. The pressure ratio is considered at a radial distance 0.02 mm below the outer surface of the artery. The radius and wall thickness of the artery are taken to be 1.0 mm and 0.1 mm, respectively, when $\omega t = \pi$. The results reveal that the pressure variation in the case of large consolidation time is much different than that, when the consolidation time is small.

of pressure with time quantitatively as well as qualitatively, it does not affect the time at which the pressure attains its maximum and the time instants at which the pressure vanishes.

The distribution of the radial velocity of the interstitial fluid in the stenosed segment of an artery, as well as an artery constricted by mechanical means, has been shown in Figure 9. It may be noted that the interstitial fluid velocity is greatly affected by the size of the stenosis (Figure 9a). This asserts that the degree of stenosis is an important factor not only in the estimation of the flow velocity of blood, but also in the determination of the interstitial fluid velocity. Figure 9b gives the velocity distribution for the situation, when in the normal artery a constriction is caused by some mechanical means. It is quite important to compare Figures 9a and 9b. Such a comparison reveals that the velocity distribution in the vicinity of a constriction caused by atherosclerotic plaques is much different from that in the neighbourhood of a constriction in a normal artery, caused by mechanical means. Figure 10 gives pressure distributions in the constricted artery where the constriction is caused either due to atherosclerosis or due to some mechanical reason, the nondimensional stenosis height being 0.1 in both cases. We notice that the pressure distributions in the two cases are entirely different. Figures 11a and 11b give the pressure

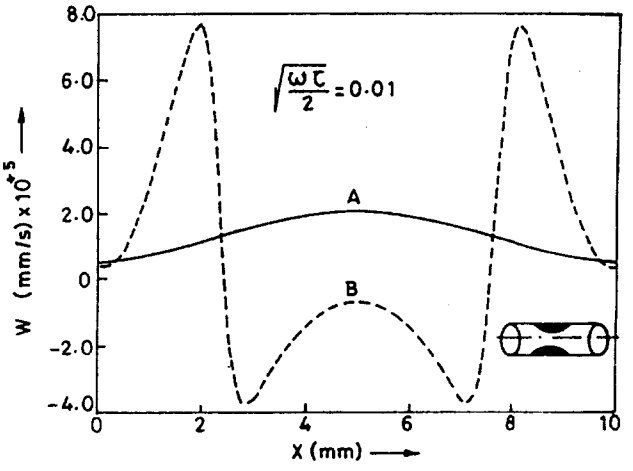

Figure 12. Plots for interstitial fluid velocity versus axial distance. The curve 'A' gives the velocity variation at points 0.01 mm above the endothelium, while the curve 'B' represents the said variation at points 0.02 mm below the outer surface of the artery. The results are computed for 20% occlusion, when $\omega t = \pi$. These figures indicate that the magnitude of the radial velocity of the interstitial fluid, as well as the nature of its variation in the axial direction, strongly depends on the site of the fluid particles.

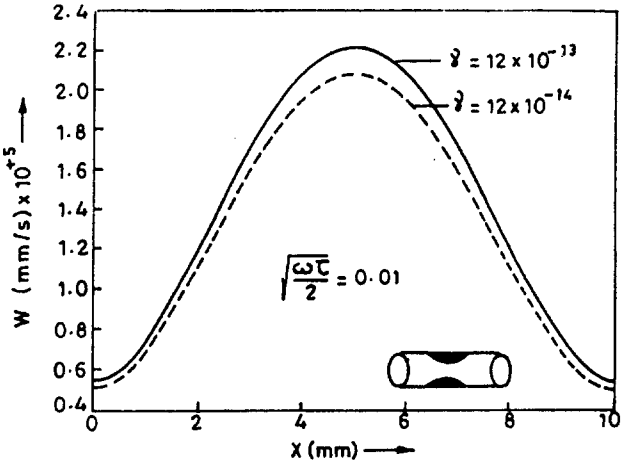

Figure 13. Variation of the radial velocity of the interstitial fluid of the stenosed artery with axial distance, for two different values of the microrotational gradient coefficient parameter (γ) of the erythrocytes of blood. The results presented by means of these curves reveal that an increase in the value of the said parameter results in an enhancement of the magnitude of the radial velocity of the interstitial fluid; however, the nature of variation along the axis of the artery is not affected by the extent of microrotation (at least within the limited range considered for the present study) of the erythrocytes.

distributions for two different stenosis sizes corresponding to two different values of consolidation time. It is observed that for small consolidation time, there occurs tremendous fluctuation of pressure (cf. Figure 11b), but if the consolidation time is large, the pressure variation takes place uniformly (Figure 11a). From Figure 12, we have an idea of the velocity distribution in the interstitial space, on the endothelial and the adventitial layers of the stenosed region of the artery. It may be noted that the interstitial fluid velocity on the adventitia of the stenosed arterial wall is of a fluctuating nature, but on the endothelium it is not so.

Figure 13 gives an estimate of the change in the interstitial fluid velocity due to a change in the rotational velocity of the erythrocytes of blood. This figure reveals that with an increase in

the rotational gradient coefficient, there is an enhancement in the interstitial fluid velocity in the radial direction of the artery in the stenosed area.

7. CONCLUDING REMARKS

The mathematical analysis presented in the paper, together with the quantitative analysis leads to some important conclusions that should be of considerable interest to clinicians, physicists, as well as bioengineers, particularly to those who are involved in the construction of artificial organs. First, the present study reveals that the microrotation of erythrocytes brings about an appreciable change in the velocity profile of blood, which in turn affects significantly the velocity distribution of the interstitial fluid in the porous matrix of the arterial wall. Second, the size of the stenosis has a strong potential to change the velocity distribution of blood, as well as that of the interstitial fluid. Also, these quantities for a constriction caused due to atherosclerotic plaques is much different from an arterial constriction in the normal artery, caused by some mechanical means. Last, we may mention our consideration (based on experimental observations) that the coarse fibers of the arterial wall which impart velocity gradients within the fine material (incorporated through the no-slip condition on the surface of the coarse fibers) is a step forward towards understanding the interstitial flow; this consideration, as the present investigation shows, is an important factor in the determination of the flow characteristics in the interstitial space.

APPENDIX I

Derived expressions for A'_T, C, M_1, C' involved in (30) and those of A, B, A', and E in equations (42) and (43),

$$C = \left[\frac{U_0 a^2 R I_0(kR)}{\psi_0}\left\{\frac{kI_1(A_{11}R) - A_{11}I_1(kR)}{(A_{11}^2 - A_{12}^2)(A_{11}^2 - k^2)}\right\} - \left(k - \frac{RU_0 a^2 I_1(kR)}{\psi_0}\right)\left\{\frac{A_{11}(I_0(kR) - I_0(A_{11}R))}{(A_{11}^2 - A_{12}^2)(A_{11}^2 - k^2)}\right\}\right] T_1^{-1},$$

$$T_1 = \left[\left\{\frac{A_{11}R}{(A_{12}^2 - k^2)}\frac{(A_{12}I_1(kR) - kI_1(A_{12}R))}{(A_{11}^2 - k^2)}\frac{(I_0(A_{11}R) - I_0(kR))}{(A_{11}^2 - A_{12}^2)}\right\} - \left\{\frac{RA_{12}}{(A_{12}^2 - k^2)}\frac{(kI_1(A_{11}R) - A_{11}I_1(kR))}{(A_{11}^2 - k^2)}\frac{(I_0(kR) - I_0(A_{12}R))}{(A_{11}^2 - A_{12}^2)}\right\}\right],$$

$$M_1 = \frac{[U_0 a^2 I_0(kR)/\psi_0 - (CA_{12}/(A_{12}^2 - k^2))\{I_0(A_{12}R) - I_0(kR)\}]}{[A_{11}(I_0(kR) - I_0(A_{11}R))]/(A_{11}^2 - A_{12}^2)(A_{11}^2 - k^2)},$$

$$A'_T = -\frac{i}{kI_0(kR)}\left\{\frac{A_{12}CI_0(A_{12}R)}{(A_{12}^2 - k^2)} - \frac{M_1 A_{11} I_0(A_{11}R)}{(A_{11}^2 - k^2)(A_{11}^2 - A_{12}^2)}\right\},$$

$$C' = \frac{2a^2}{B_{11}I_0(B_{11}R)}\left[\frac{CA_{12}}{\gamma}\frac{I_0(A_{12}R)}{(A_{12}^2 - B_{11}^2)} - \frac{M_1 A_{11} I_0(A_{11}R)}{\gamma(A_{11}^2 - A_{12}^2)(A_{11}^2 - B_{11}^2)}\right],$$

$$A' = RV_T,$$

$$A = \frac{A'(V_{N3}V_B - V_{N2}(H_2\delta^2/R_1^2 H_1)(\lambda\nu^*/2G - 1)) - V_{N4}V_B}{V_A V_{N2} - V_{N1}V_B},$$

$$B = \frac{V_{N4} - A'V_{N3} - AV_{N1}}{V_{N2}},$$

$$E = -\frac{H_4}{H_1 H_3}\left\{\left\{AI_0\left(H_1\frac{R_1}{\delta}\right) + BK_0\left(H_1\frac{R_1}{\delta}\right)\right\} + A'\frac{(H_2H_4 - H_5)}{H_4}\log\left(\frac{R_1}{\delta}\right)\right\},$$

$$K = -P_C - \frac{2a^3 G H_1}{\psi_0 \mu\delta\nu^*}\left[AV_{B1} + BV_{B1} + \frac{A'H_2\delta^2}{R^2 H_1}\left(\frac{\lambda\nu^*}{2G} - 1\right)\right] + V_C\frac{2(\mu_s + \mu_r)}{\mu},$$

$$P_C = \frac{1}{\mu}\left[\{-k\alpha^2 A'_T(\mu_s+\mu_r)I_0(kR)\} + C\left\{\frac{ki\alpha^2(\mu_s+\mu_r)I_0(A_{12}R)}{A_{12}(A_{12}^2-k^2)}\right.\right.$$
$$\left. + k(\mu_s+\mu_r)i\frac{I_0(A_{12}R)}{A_{12}} - \frac{4ik\mu_r^2}{\gamma A_{12}}\frac{I_0(A_{12}R)}{(A_{12}^2-B_{11}^2)}\right\}$$
$$+ \frac{M_1}{A_{11}(A_{11}^2-A_{12}^2)}\left\{\frac{-\alpha^2 k(\mu_s+\mu_r)iI_0(A_{11}R)}{(A_{11}^2-k^2)} - ik(\mu_r+\mu_s)I_0(A_{11}R)\right.$$
$$\left. + \frac{4i\mu_r^2 k}{\gamma}\frac{I_0(A_{11}R)}{(A_{11}^2-B_{11}^2)}\right\} + C'\frac{2\mu_r ik}{B_{11}}I_0(B_{11}R)\Bigg],$$

$$V_c = kA'_T\left(I_0(kR) - \frac{I_1(kR)}{kR}\right) - \frac{iCkA_{12}}{(A_{12}^2-k^2)}\left(I_0(A_{12}R) - \frac{I_1(A_{12}R)}{A_{12}R}\right)$$
$$+ \frac{ikM_1A_{11}}{(A_{11}^2-A_{12}^2)(A_{11}^2-k^2)}\left(I_0(A_{11}R) - \frac{I_1(A_{11}R)}{A_{11}R}\right),$$

$$V_T = k\left\{-A'_T I_1(kR) + Ci\frac{I_1(A_{12}R)}{(A_{12}^2-k^2)} - \frac{iM_1I_1(A_{11}R)}{(A_{11}^2-A_{12}^2)(A_{11}^2-k^2)}\right\},$$

$$V_A = I_0\left(H_1(R_1/\delta)\right) - \frac{\delta I_1\left(H_1(R_1/\delta)\right)}{R_1} + \frac{\nu^*\lambda}{H_1 2G}\frac{\delta I_1\left(H_1(R_1/\delta)\right)}{R_1},$$

$$V_B = K_0\left(H_1(R_1/\delta)\right) - \frac{\delta K_1\left(H_1(R_1/\delta)\right)}{R_1} + \frac{\nu^*\lambda}{H_1 2G}\frac{\delta K_1\left(H_1(R_1/\delta)\right)}{R_1},$$

$$V_{A1} = I_0\left(H_1(R/\delta)\right) - \frac{\delta I_1\left(H_1(R/\delta)\right)}{R} + \frac{\nu^*\lambda}{H_1 2G}\frac{\delta I_1\left(H_1(R/\delta)\right)}{R},$$

$$V_{B1} = K_0\left(H_1(R/\delta)\right) - \frac{\delta K_1\left(H_1(R/\delta)\right)}{R} + \frac{\nu^*\lambda}{H_1 2G}\frac{\delta K_1\left(H_1(R/\delta)\right)}{R},$$

$$V_{N1} = V_{A1}\frac{H_1H_3}{H_4} + \frac{\psi_0\mu\delta\nu^*}{H_1 2Ga^3}\left(I_0\left(H_1\frac{R}{\delta}\right) - I_0\left(H_1\frac{R_1}{\delta}\right)\right),$$

$$V_{N2} = \frac{V_{B1}H_1H_3}{H_4} + \frac{\psi_0\mu\delta\nu^*}{H_1 2Ga^3}\left(K_0\left(H_1\frac{R}{\delta}\right) - K_0\left(H_1\frac{R_1}{\delta}\right)\right),$$

$$V_{N3} = \left(\frac{\lambda\nu^*}{2G} - 1\right)\frac{H_2H_3\delta^2}{H_4R^2} + \frac{\mu\delta\nu^*}{2Ga^3H_1}\frac{(H_4H_2 - H_5)}{H_4}\log\frac{R}{R_1},$$

$$V_{N4} = \frac{\psi_0\delta H_3\nu^*}{H_4 a^3 2G}(\mu_s+\mu_r)V_C.$$

APPENDIX II

Derived expressions for various symbols appearing in equations (44) and (45):

$$A_1 = \frac{(A_{k1}+A_{k2}-A_{k3})T_{k1} + (A_{k4}-A_{k5}+A_{k6})T_{k2}}{T_{k1}^2+T_{k2}^2},$$

$$A_2 = \frac{-(A_{k1}+A_{k2}-A_{k3})T_{k2} + (A_{k4}-A_{k5}+A_{k6})T_{k1}}{T_{k1}^2+T_{k2}^2},$$

$$B_1 = \frac{B_{k1}V_{N21} + B_{k2}V_{N22}}{V_{N1}^2+V_{N2}^2},$$

$$B_2 = \frac{B_{k2}V_{N21} - B_{k1}V_{N22}}{V_{N1}^2+V_{N2}^2},$$

$$A'_1 = RV_{T1},$$

$$A'_2 = RV_{T2},$$

$$E_1 = -H_c[A_1 I_{101} - A_2 I_{102} + B_1 K_{101} - B_2 K_{102}] + H_d[A_1 I_{102} + I_{101} A_2 + B_1 K_{102} + B_2 K_{101}]$$
$$- (A_1' h_{p31} - A_2' h_{p32}) \log X + \tan^{-1} \frac{h_{12}}{h_{11}} (A_2' h_{p31} + A_1' h_{p32}),$$

$$E_2 = -H_c[A_1 I_{102} + A_2 I_{101} + B_1 K_{102} + B_2 K_{101}] - H_d[A_1 I_{101} - I_{102} A_2 + B_1 K_{101} - B_2 K_{102}]$$
$$- (A_1' h_{p31} - A_2' h_{p32}) \tan^{-1} \frac{h_{12}}{h_{11}} - \log X (A_2' h_{p31} + A_1' h_{p32}),$$

where

$$A_{k1} = A_1'(V_{N31} V_{B21} - V_{B22} V_{N32} + V_{N21} H_{z31} - V_{N22} H_{z32}),$$
$$A_{k2} = V_{N42} V_{B22} - V_{N41} V_{B21},$$
$$A_{k3} = A_2'(V_{B21} V_{N32} + V_{B22} V_{N31} + V_{N21} H_{z32} + V_{N22} H_{z31}),$$
$$A_{k4} = A_1'(V_{N32} V_{B21} + V_{B22} V_{N31} + V_{N21} H_{z32} + V_{N22} H_{z31}),$$
$$A_{k5} = V_{N41} V_{B22} + V_{N42} V_{B21},$$
$$A_{k6} = A_2'(V_{B21} V_{N31} - V_{B22} V_{N32} + V_{N21} H_{z31} - V_{N22} H_{z32}),$$
$$B_{k1} = A_2 V_{N12} - A_1 V_{N11} + V_{N41} + A_2' V_{N32} - A_1' V_{N31},$$
$$B_{k2} = V_{N42} - A_1 V_{N12} - A_2 V_{N11} - A_1' V_{N32} - A_2' V_{N31},$$

$$V_{N31} = \frac{Y_{11} a^2}{R^2} \frac{\lambda \nu^*}{2G} \frac{H_2 h^2 (h_{11}^2 - h_{12}^2)}{(h_{11}^2 - h_{12}^2)^2 + 4 h_{11}^2 h_{12}^2} - \frac{Y_{12} a^2}{R^2} \left(\frac{\lambda \nu^*}{2G} - 1 \right) \frac{2 H_2 h^2 h_{11} h_{12}}{(h_{11}^2 - h_{12}^2)^2 + 4 h_{11}^2 h_{12}^2}$$
$$+ \frac{\mu \nu^*}{2 G a^3} \log \frac{R}{R_1} \frac{h_{p31} h_{11} + h_{p32} h_{12}}{h_{11}^2 + h_{12}^2},$$

$$V_{N32} = \frac{Y_{12} a^2}{R^2} \frac{\lambda \nu^*}{2G} \frac{H_2 h^2 (h_{11}^2 - h_{12}^2)}{(h_{11}^2 - h_{12}^2)^2 + 4 h_{11}^2 h_{12}^2} - \frac{Y_{11} a^2}{R^2} \left(\frac{\lambda \nu^*}{2G} - 1 \right) \frac{2 H_2 h^2 h_{11} h_{12}}{(h_{11}^2 - h_{12}^2)^2 + 4 h_{11}^2 h_{12}^2}$$
$$+ \frac{\nu^* \mu}{2 G a^3} \log \frac{R}{R_1} \frac{h_{p32} h_{11} - h_{p31} h_{12}}{h_{11}^2 + h_{12}^2},$$

$$V_{N41} = \frac{\psi_0 \nu^* h^2 (\mu_s + \mu_r) a}{G \left((h_{11}^2 - h_{12}^2)^2 + 4 h_{11}^2 h_{12}^2 \right)} (Y_{11} V_{c1} - Y_{12} V_{c2}) h_{11}$$
$$+ \frac{\psi_0 \nu^* h^2 (\mu_s + \mu_r) a}{G \left((h_{11}^2 - h_{12}^2)^2 + 4 h_{11}^2 h_{12}^2 \right)} (Y_{12} V_{c1} + Y_{11} V_{c2}) h_{12},$$

$$V_{N42} = \frac{-\psi_0 \nu^* h^2 (\mu_s + \mu_r) a}{G (h_{11}^2 + h_{12}^2)^2 + 4 h_{11}^2 h_{12}^2} (Y_{11} V_{c1} - Y_{12} V_{c2}) h_{12}$$
$$+ \frac{\psi_0 \nu^* h^2 (\mu_s + \mu_r) a}{G \left((h_{11}^2 - h_{12}^2)^2 + 4 h_{11}^2 h_{12}^2 \right)} (Y_{12} V_{c1} + Y_{11} V_{c2}) h_{11},$$

$$h_{p11} = \left(1 + k^2 \beta K_p - \frac{H_2 K_p \beta h_{11}}{h} \right),$$

$$h_{p12} = \frac{H_2 K_p \beta h_{12}}{h},$$

$$t_3 = a^2 (1 + \beta k^2 K_p),$$

$$t_4 = -\frac{G k^2 K_p a^2}{\mu \omega},$$

$$h_{p21} = t_3 - \frac{\beta K_p}{h} (t_3 (h_{11}^2 - h_{12}^2) - 2 t_4 h_{11} h_{12}),$$

$$h_{p22} = \frac{\beta K_p}{h^2}\left(2t_3 h_{11}h_{12} + t_4\left(h_{11}^2 - h_{12}^2\right)\right),$$

$$h_{p31} = \frac{t_3}{a^2} - \left(h_{p11}h_{21} + h_{p12}h_{p22}\right),$$

$$h_{p32} = \left(h_{p11}h_{22} - h_{p12}h_{p21}\right),$$

$$F_{11} = h^2\left(\frac{\lambda\nu^*}{2G} - 1\right)\frac{H_2 h_{21}}{R_1^2\left(h_{21}^2 + h_{22}^2\right)}a^2,$$

$$F_{12} = h^2\left(\frac{\lambda\nu^*}{2G} - 1\right)\frac{H_2 h_{22}}{R_1^2\left(h_{21}^2 + h_{22}^2\right)}a^2,$$

$$H_{z31} = \frac{F_{11}\left(h_{11}^2 - h_{12}^2\right) - 2F_{12}h_{11}h_{12}}{\left(h_{11}^2 - h_{12}^2\right)^2 + 4h_{11}^2h_{12}^2},$$

$$H_{z32} = \frac{F_{12}\left(h_{11}^2 - h_{12}^2\right) - 2F_{11}h_{11}h_{12}}{\left(h_{11}^2 - h_{12}^2\right)^2 + 4h_{11}^2h_{12}^2},$$

$$H_{c1} = a^2\left(\beta k^2 K_p + 1\right) - \frac{\beta K_p}{R^2}\left(h_{31}^2 - h_{32}^2\right),$$

$$H_{c2} = \frac{2\beta K_p H_2^2 h_{31}h_{32}}{R^2},$$

$$H_{c31} = \frac{\psi_0\mu}{2a^3\lambda G}\frac{\left(\left(1 - \beta K_p h_{11}/h\right)h_{21} + \beta K_p h_{12}h_{22}/h\right)}{\left(h_{21}^2 + h_{22}^2\right)},$$

$$H_{c41} = \frac{\left(\left(1 - \beta K_p h_{11}/h\right)h_{22} - \beta K_p h_{12}h_{21}/h\right)}{\left(h_{21}^2 + h_{22}^2\right)},$$

$$H_{c3} = \frac{H_{c31}h_{11} + H_{c41}h_{12}}{h_{11}^2 + h_{12}^2},$$

$$H_{c4} = \frac{H_{c41}h_{11} - H_{c31}h_{12}}{h_{11}^2 + h_{12}^2},$$

$$H_c = \frac{H_{c1}H_{c3} + H_{c2}H_{c4}}{H_{c3}^2 + H_{c4}^2},$$

$$H_d = \frac{H_{c2}H_{c3} - H_{c1}H_{c4}}{H_{c3}^2 + H_{c4}^2},$$

$$X = R\sqrt{h_{11}^2 + h_{12}^2},$$

$$Y = r\sqrt{h_{11}^2 + h_{12}^2},$$

$$V_{N11} = V_{A11}Z_{11} - V_{A12}Z_{12} + \frac{h\psi_0\mu\nu^* h_{21}}{2a^3G\left(h_{21}^2 + h_{22}^2\right)}\frac{\left(I_{01} - I_{101}\right)h_{11} + h_{12}\left(I_{02} - I_{102}\right)}{h_{11}^2 + h_{12}^2}$$
$$+ \frac{h\psi_0\mu\nu^* h_{22}}{2a^3G\left(h_{21}^2 + h_{22}^2\right)}\frac{-\left(I_{01} - I_{101}\right)h_{12} + h_{11}\left(I_{02} - I_{102}\right)}{h_{11}^2 + h_{12}^2},$$

$$V_{N12} = V_{A11}Z_{12} + V_{A12}Z_{11} - \frac{h\psi_0\mu\nu^* h_{22}}{2a^3G\left(h_{21}^2 + h_{22}^2\right)}\frac{\left(I_{01} - I_{101}\right)h_{11} + h_{12}\left(I_{02} - I_{102}\right)}{h_{11}^2 + h_{12}^2}$$
$$+ \frac{\psi_0 h\mu\nu^* h_{21}}{2a^3G\left(h_{21}^2 + h_{22}^2\right)}\frac{-\left(I_{01} - I_{101}\right)h_{12} + h_{11}\left(I_{02} - I_{102}\right)}{h_{11}^2 + h_{12}^2},$$

$$V_{N21} = V_{B11}Z_{11} - V_{B12}Z_{12} + \frac{h\psi_0\mu\nu^* h_{21}}{2a^3G\left(h_{21}^2 + h_{22}^2\right)}\frac{\left(K_{01} - K_{101}\right)h_{11} + h_{12}\left(K_{02} - K_{102}\right)}{h_{11}^2 + h_{12}^2}$$

$$+\frac{\psi_0 h\mu\nu^* h_{22}}{2a^3G(h_{21}^2+h_{22}^2)}\frac{-(K_{01}-K_{101})h_{12}+h_{11}(K_{02}-K_{102})}{h_{11}^2+h_{12}^2},$$

$$V_{N22}=V_{B11}Z_{12}+V_{B12}Z_{11}-\frac{h\psi_0\mu\nu^* h_{22}}{2a^3G(h_{21}^2+h_{22}^2)}\frac{(K_{01}-K_{101})h_{11}+h_{12}(K_{02}-K_{102})}{h_{11}^2+h_{12}^2}$$
$$+\frac{\psi_0 h\mu\nu^* h_{21}}{2a^3G(h_{21}^2+h_{22}^2)}\frac{-(K_{01}-K_{101})h_{12}+h_{11}(K_{02}-K_{102})}{h_{11}^2+h_{12}^2},$$

$$V_{T2}=C\frac{I_1(A_{12}R)}{A_{12}^2-k^2}-\frac{M_1 I_1(A_{11}R)}{(A_{11}^2-A_{12}^2)(A_{11}^2-k^2)},$$

$$V_{T1}=-A_T' kI_1(kR),$$

$$H_{z11}=\frac{h}{R}\left(1-\frac{\lambda\nu^* h_{21}}{2G(h_{21}^2+h_{22}^2)}\right),$$

$$H_{z12}=-\frac{\lambda\nu^* h_{22}}{2G(h_{21}^2+h_{22}^2)},$$

$$H_{z21}=\frac{h}{R_1}\left(1-\frac{\lambda\nu^* h_{21}}{2G(h_{21}^2+h_{22}^2)}\right),$$

$$H_{z22}=-\frac{\lambda\nu^* h_{22}}{2G(h_{21}^2+h_{22}^2)},$$

$$V_{A21}=I_{101}-H_{z21}\frac{(I_{111}h_{11}+I_{112}h_{12})}{h_{12}^2+h_{11}^2}+H_{z22}\frac{-I_{111}h_{12}+I_{112}h_{11}}{h_{12}^2+h_{11}^2},$$

$$V_{A22}=I_{102}-H_{z22}\frac{(I_{111}h_{11}+I_{112}h_{12})}{h_{12}^2+h_{11}^2}-H_{z21}\frac{-I_{111}h_{12}+I_{112}h_{11}}{h_{12}^2+h_{11}^2},$$

$$V_{B21}=K_{101}-H_{z21}\frac{K_{111}h_{11}+K_{112}h_{12}}{h_{12}^2+h_{11}^2}+H_{z22}\frac{-K_{111}h_{12}+k_{112}h_{11}}{h_{12}^2+h_{11}^2},$$

$$V_{B22}=K_{102}-H_{z22}\frac{K_{111}h_{11}+K_{112}h_{12}}{h_{12}^2+h_{11}^2}-H_{z21}\frac{-K_{111}h_{12}+K_{112}h_{11}}{h_{12}^2+h_{11}^2},$$

$$V_{A11}=I_{01}-H_{z11}\frac{I_{11}h_{11}+I_{12}h_{12}}{h_{12}^2+h_{11}^2}+H_{z12}\frac{-I_{11}h_{12}+I_{12}h_{11}}{h_{12}^2+h_{11}^2},$$

$$V_{A12}=I_{02}-H_{z12}\frac{I_{11}h_{11}+I_{12}h_{12}}{h_{12}^2+h_{11}^2}-H_{z11}\frac{-I_{11}h_{12}+I_{12}h_{11}}{h_{12}^2+h_{11}^2},$$

$$V_{B11}=K_{01}+H_{z11}\frac{K_{11}h_{11}+K_{12}h_{12}}{h_{12}^2+h_{11}^2}+H_{z12}\frac{-K_{11}h_{12}+K_{12}h_{11}}{h_{12}^2+h_{11}^2},$$

$$V_{B12}=K_{02}-H_{z12}\frac{K_{11}h_{11}+K_{12}h_{12}}{h_{12}^2+h_{11}^2}-H_{z11}\frac{-K_{11}h_{12}+K_{12}h_{11}}{h_{12}^2+h_{11}^2},$$

(h_{11},h_{12}), (h_{21},h_{22}), (P_{c1},P_{c2}), (V_{c1},V_{c2}), (Z_{11},Z_{12}), (Y_{11},Y_{12}) are the real and imaginary parts of

$$\left(\frac{\beta K_p\omega^2 r^2/h^2+i\omega\tau}{(\beta K_p\omega\tau/h^2)^2+1}\right)^{1/2},a\left(1+\beta k^2K_p-i\frac{Gk^2K_p}{\omega\mu}\right),P_C,V_c,\frac{H_1H_3}{H_4},\frac{H_3}{H_4},$$

$$h_{31}=\frac{R}{h}(h_{11}h_{21}-h_{22}h_{12}),$$

$$h_{32}=\frac{R}{h}(h_{12}h_{21}+h_{22}h_{11}),$$

$$h_{33}=\frac{R_1}{h}(h_{11}h_{21}-h_{22}h_{12}),$$

$$h_{34}=\frac{R_1}{h}(h_{12}h_{21}+h_{22}h_{11}),$$

$$h_{35} = \frac{r}{h}(h_{11}h_{21} - h_{22}h_{12}),$$

$$h_{36} = \frac{r}{h}(h_{12}h_{21} + h_{22}h_{11}),$$

$$\theta_1 = \tan^{-1}\frac{h_{32}}{h_{31}},$$

$$b_2 = \sqrt{(h_{31}^2 + h_{32}^2)},$$

$$b_3 = \sqrt{(h_{33}^2 + h_{34}^2)},$$

$$b_4 = \sqrt{(h_{35}^2 + h_{36}^2)},$$

$$I_{01} = \frac{e^{h_{31}}}{\sqrt{2\pi b_2}}\left(\cos(h_{32})\cos\left(\frac{\theta_1}{2}\right) + \sin(h_{32})\sin\left(\frac{\theta_1}{2}\right)\right) \times \left(1 + \frac{\cos(\theta_1)}{8b_2} + \frac{1.9\cos(2\theta_1)}{2!8^2b_2^2} + \frac{1.9.25\cos(3\theta_1)}{3!8^3b_2^3} + \cdots\right),$$

$$I_{02} = \frac{e^{h_{31}}}{\sqrt{2\pi b_2}}\left(-\cos(h_{32})\sin\left(\frac{\theta_1}{2}\right) + \sin(h_{32})\cos\left(\frac{\theta_1}{2}\right)\right) \times \left(\frac{\sin(\theta_1)}{8b_2} + \frac{1.9\sin(2\theta_1)}{2!8^2b_2^2} + \frac{1.9.25\sin(3\theta_1)}{3!8^3b_2^3} + \cdots\right),$$

$$K_{01} = \frac{\pi e^{-h_{31}}}{\sqrt{2b_2}}\left(\cos(h_{32})\cos\left(\frac{\theta_1}{2}\right) - \sin(h_{32})\sin\left(\frac{\theta_1}{2}\right)\right) \times \left(1 - \frac{\cos(\theta_1)}{8b_2} + \frac{1.9\cos(2\theta_1)}{2!8^2b_2^2} - \frac{1.9.25\cos(3\theta_1)}{3!8^3b_2^3} + \cdots\right),$$

$$K_{02} = \frac{\pi e^{h_{31}}}{\sqrt{2b_2}}\left(\cos(h_{32})\sin\left(\frac{\theta_1}{2}\right) + \sin(h_{32})\cos\left(\frac{\theta_1}{2}\right)\right) \times \left(\frac{\sin(\theta_1)}{8b_2} - \frac{1.9\sin(2\theta_1)}{2!8^2b_2^2} + \frac{1.9.25\sin(3\theta_1)}{3!8^3b_2^3} - \cdots\right),$$

$$I_{101} = \frac{e^{h_{33}}}{\sqrt{2\pi b_3}}\left(\cos(h_{34})\cos\left(\frac{\theta_1}{2}\right) + \sin(h_{34})\sin\left(\frac{\theta_1}{2}\right)\right) \times \left(1 + \frac{\cos(\theta_1)}{8b_3} + \frac{1.9\cos(2\theta_1)}{2!8^2b_3^2} + \frac{1.9.25\cos(3\theta_1)}{3!8^3b_3^3} + \cdots\right),$$

$$I_{102} = \frac{e^{h_{33}}}{\sqrt{2\pi b_3}}\left(-\cos(h_{34})\sin\left(\frac{\theta_1}{2}\right) + \sin(h_{34})\cos\left(\frac{\theta_1}{2}\right)\right) \times \left(\frac{\sin(\theta_1)}{8b_3} + \frac{1.9\sin(2\theta_1)}{2!8^2b_3^2} + \frac{1.9.25\sin(3\theta_1)}{3!8^3b_3^3} + \cdots\right),$$

$$K_{101} = \frac{\pi e^{-h_{33}}}{\sqrt{2b_3}}\left(\cos(h_{34})\cos\left(\frac{\theta_1}{2}\right) - \sin(h_{34})\sin\left(\frac{\theta_1}{2}\right)\right) \times \left(1 - \frac{\cos(\theta_1)}{8b_3} + \frac{1.9\cos(2\theta_1)}{2!8^2b_3^2} - \frac{1.9.25\cos(3\theta_1)}{3!8^3b_3^3} + \cdots\right),$$

$$K_{102} = \frac{\pi e^{h_{33}}}{\sqrt{2b_3}}\left(\cos(h_{34})\sin\left(\frac{\theta_1}{2}\right) + \sin(h_{34})\cos\left(\frac{\theta_1}{2}\right)\right) \times \left(\frac{\sin(\theta_1)}{8b_3} - \frac{1.9\sin(2\theta_1)}{2!8^2b_3^2} + \frac{1.9.25\sin(3\theta_1)}{3!8^3b_3^3} - \cdots\right),$$

$$I_{11} = \frac{e^{h_{31}}}{\sqrt{2\pi b_2}}\left(\cos(h_{32})\cos\left(\frac{\theta_1}{2}\right) + \sin(h_{32})\sin\left(\frac{\theta_1}{2}\right)\right)$$

$$\times\left(1-\frac{3\cos(\theta_1)}{8b_2}+\frac{1.15.\cos(2\theta_1)}{2!8^2b_2^2}+\frac{1.15.21\cos(3\theta_1)}{3!8^3b_2^3}+\cdots\right),$$

$$I_{12}=\frac{e^{h_{31}}}{\sqrt{2\pi b_2}}\left(\cos(h_{32})\sin\left(\frac{\theta_1}{2}\right)-\sin(h_{32})\cos\left(\frac{\theta_1}{2}\right)\right)$$
$$\times\left(\frac{3\sin(\theta_1)}{8b_2}+\frac{1.15.\sin(2\theta_1)}{2!8^2b_2^2}+\frac{1.15.21.\sin(3\theta_1)}{3!8^3b_2^3}+\cdots\right),$$

$$K_{11}=\frac{\pi e^{-h_{31}}}{\sqrt{2b_2}}\left(\cos(h_{32})\cos\left(\frac{\theta_1}{2}\right)-\sin(h_{32})\sin\left(\frac{\theta_1}{2}\right)\right)$$
$$\times\left(1-\frac{3\cos(\theta_1)}{8b_2}+\frac{1.15\cos(2\theta_1)}{2!8^2b_2^2}-\frac{1.15.21.\cos(3\theta_1)}{3!8^3b_2^3}+\cdots\right),$$

$$K_{12}=\frac{\pi e^{h_{31}}}{\sqrt{2b_2}}\left(\cos(h_{32})\sin\left(\frac{\theta_1}{2}\right)+\sin(h_{32})\cos\left(\frac{\theta_1}{2}\right)\right)$$
$$\times\left(\frac{3\sin(\theta_1)}{8b_2}-\frac{1.15.\sin(2\theta_1)}{2!8^2b_2^2}+\frac{1.15.21.\sin(3\theta_1)}{3!8^3b_2^3}-\cdots\right),$$

$$I_{111}=\frac{e^{h_{33}}}{\sqrt{2\pi b_3}}\left(\cos(h_{34})\cos\left(\frac{\theta_1}{2}\right)+\sin(h_{34})\sin\left(\frac{\theta_1}{2}\right)\right)$$
$$\times\left(1-\frac{3\cos(\theta_1)}{8b_3}+\frac{1.15.\cos(2\theta_1)}{2!8^2b_3^2}+\frac{1.15.21\cos(3\theta_1)}{3!8^3b_3^3}+\cdots\right),$$

$$I_{112}=\frac{e^{h_{33}}}{\sqrt{2\pi b_2}}\left(\cos(h_{34})\sin\left(\frac{\theta_1}{2}\right)-\sin(h_{34})\cos\left(\frac{\theta_1}{2}\right)\right)$$
$$\times\left(\frac{3\sin(\theta_1)}{8b_3}+\frac{1.15.\sin(2\theta_1)}{2!8^2b_3^2}+\frac{1.15.21.\sin(3\theta_1)}{3!8^3b_3^3}+\cdots\right),$$

$$K_{111}=\frac{\pi e^{-h_{33}}}{\sqrt{2b_3}}\left(\cos(h_{34})\cos\left(\frac{\theta_1}{2}\right)-\sin(h_{34})\sin\left(\frac{\theta_1}{2}\right)\right)$$
$$\times\left(1-\frac{3\cos(\theta_1)}{8b_3}+\frac{1.15\cos(2\theta_1)}{2!8^2b_3^2}-\frac{1.15.21.\cos(3\theta_1)}{3!8^3b_3^3}+\cdots\right),$$

$$K_{112}=\frac{\pi e^{h_{33}}}{\sqrt{2b_3}}\left(\cos(h_{34})\sin\left(\frac{\theta_1}{2}\right)+\sin(h_{34})\cos\left(\frac{\theta_1}{2}\right)\right)$$
$$\times\left(\frac{3\sin(\theta_1)}{8b_3}-\frac{1.15.\sin(2\theta_1)}{2!8^2b_3^2}+\frac{1.15.21.\sin(3\theta_1)}{3!8^3b_3^3}-\cdots\right),$$

$$I_{r01}=\frac{e^{h_{35}}}{\sqrt{2\pi b_4}}\left(\cos(h_{36})\cos\left(\frac{\theta_1}{2}\right)+\sin(h_{36})\sin\left(\frac{\theta_1}{2}\right)\right)$$
$$\times\left(1+\frac{\cos(\theta_1)}{8b_4}+\frac{1.9\cos(2\theta_1)}{2!8^2b_4^2}+\frac{1.9.25\cos(3\theta_1)}{3!8^3b_4^3}+\cdots\right),$$

$$I_{r02}=\frac{e^{h_{35}}}{\sqrt{2\pi b_4}}\left(-\cos(h_{36})\sin\left(\frac{\theta_1}{2}\right)+\sin(h_{36})\cos\left(\frac{\theta_1}{2}\right)\right)$$
$$\times\left(\frac{\sin(\theta_1)}{8b_4}+\frac{1.9\sin(2\theta_1)}{2!8^2b_4^2}+\frac{1.9.25\sin(3\theta_1)}{3!8^3b_4^3}+\cdots\right),$$

$$K_{r01}=\frac{\pi e^{-h_{35}}}{\sqrt{2b_4}}\left(\cos(h_{36})\cos\left(\frac{\theta_1}{2}\right)-\sin(h_{36})\sin\left(\frac{\theta_1}{2}\right)\right)$$
$$\times\left(1-\frac{\cos(\theta_1)}{8b_4}+\frac{1.9\cos(2\theta_1)}{2!8^2b_4^2}-\frac{1.9.25\cos(3\theta_1)}{3!8^3b_4^3}+\cdots\right),$$

$$K_{r02}=\frac{\pi e^{h_{35}}}{\sqrt{2b_4}}\left(\cos(h_{36})\sin\left(\frac{\theta_1}{2}\right)+\sin(h_{36})\cos\left(\frac{\theta_1}{2}\right)\right)$$

$$\times\left(\frac{\sin(\theta_1)}{8b_4}-\frac{1.9\sin(2\theta_1)}{2!8^2b_4^2}+\frac{1.9.25\sin(3\theta_1)}{3!8^3b_4^3}-\cdots\right),$$

$$I_{r1}=\frac{e^{h_{35}}}{\sqrt{2\pi b_4}}\left(\cos(h_{36})\cos\left(\frac{\theta_1}{2}\right)+\sin(h_{36})\sin\left(\frac{\theta_1}{2}\right)\right)$$
$$\times\left(1-\frac{3\cos(\theta_1)}{8b_4}+\frac{1.15.\cos(2\theta_1)}{2!8^2b_4^2}+\frac{1.15.21\cos(3\theta_1)}{3!8^3b_4^3}+\cdots\right),$$

$$I_{r2}=\frac{e^{h_{35}}}{\sqrt{2\pi b_4}}\left(\cos(h_{36})\sin\left(\frac{\theta_1}{2}\right)-\sin(h_{36})\cos\left(\frac{\theta_1}{2}\right)\right)$$
$$\times\left(\frac{3\sin(\theta_1)}{8b_4}+\frac{1.15.\sin(2\theta_1)}{2!8^2b_4^2}+\frac{1.15.21.\sin(3\theta_1)}{3!8^3b_4^3}+\cdots\right),$$

$$K_{r1}=\frac{\pi e^{-h_{35}}}{\sqrt{2b_4}}\left(\cos(h_{36})\cos\left(\frac{\theta_1}{2}\right)-\sin(h_{36})\sin\left(\frac{\theta_1}{2}\right)\right)$$
$$\times\left(1-\frac{3\cos(\theta_1)}{8b_4}+\frac{1.15\cos(2\theta_1)}{2!8^2b_4^2}-\frac{1.15.21.\cos(3\theta_1)}{3!8^3b_4^3}+\cdots\right),$$

$$K_{r2}=\frac{\pi e^{-h_{35}}}{\sqrt{2b_4}}\left(\cos(h_{36})\sin\left(\frac{\theta_1}{2}\right)+\sin(h_{36})\cos\left(\frac{\theta_1}{2}\right)\right)$$
$$\times\left(\frac{3\sin(\theta_1)}{8b_4}-\frac{1.15.\sin(2\theta_1)}{2!8^2b_4^2}+\frac{1.15.21.\sin(3\theta_1)}{3!8^3b_4^3}-\cdots\right).$$

APPENDIX III

Derived expressions for various symbols appearing in equations (46) and (47). Some symbols used here have been defined in Appendix II.

$$A_{1s}=\frac{(A_{sk1}+A_{sk2}-A_{sk3})T_{sk1}+(A_{sk4}-A_{sk5}+A_{sk6})T_{sk2}}{T_{sk1}^2+T_{sk2}^2},$$

$$A_{2s}=\frac{-(A_{sk1}+A_{sk2}-A_{sk3})T_{sk2}+(A_{sk4}-A_{sk5}+A_{sk6})T_{sk1}}{T_{sk1}^2+T_{sk2}^2},$$

$$B_{1s}=\frac{B_{sk1}V_{sN21}+B_{sk2}V_{sN22}}{V_{sN1}^2+V_{sN2}^2},$$

$$B_{2s}=\frac{B_{sk2}V_{sN21}-B_{sk1}V_{sN22}}{V_{sN1}^2+V_{sN2}^2},$$

$$A'_{1s}=RV_{T1},$$

$$A'_{2s}=RV_{T2},$$

$$E_{1s}=-H_c[A_{1s}I_{s101}-A_{2s}I_{s102}+B_{1s}K_{s101}-B_{2s}K_{s102}]+H_d[A_{1s}I_{s102}+I_{s101}A_{2s}+B_{1s}K_{s102}$$
$$+B_{2s}K_{s101}]-(A'_{1s}h_{p31}-A'_{2s}h_{p32})\log X+\tan^{-1}\frac{h_{12}}{h_{11}}(A'_{2s}h_{p31}+A'_{1s}h_{p32}),$$

$$E_{2s}=-H_c[A_{1s}I_{s102}+A_{2s}I_{s101}+B_{1s}K_{s102}+B_{2s}K_{s101}]-H_d[A_{1s}I_{s101}-I_{s102}A_{2s}+B_{1s}K_{s101}$$
$$-B_{2s}K_{s102}]-(A'_{1s}h_{p31}-A'_{2s}h_{p32})\tan^{-1}\frac{h_{12}}{h_{11}}-\log X\,(A'_{2s}h_{p31}+A'_{1s}h_{p32}),$$

where

$$A_{sk1}=A'_1(V_{N31}V_{sB21}-V_{sB22}V_{N32}+V_{sN21}H_{z31}-V_{sN22}H_{z32}),$$
$$A_{sk2}=V_{sN42}V_{sB22}-V_{sN41}V_{sB21},$$
$$A_{sk3}=-A'_{2s}(V_{sB21}V_{N32}+V_{sB22}V_{N31}+V_{sN21}H_{z32}+V_{sN22}H_{z31}),$$

$$A_{sk4} = A'_{1s}(V_{N32}V_{sB21} + V_{sB22}V_{N31} + V_{sN21}H_{z32} + V_{sN22}H_{z31}),$$

$$A_{sk5} = V_{sN41}V_{sB22} + V_{sN42}V_{sB21},$$

$$A_{sk6} = A'_{2s}(V_{sB21} + V_{N31} - V_{sB22}V_{N32} + V_{sN21}H_{z31} - V_{sN22}H_{z32}),$$

$$B_{sk1} = A_{2s}V_{sN12} - A_{1s}V_{sN11} + V_{sN41} + A'_{2s}V_{N32} - A_{1s}V_{N31},$$

$$B_{sk2} = V_{sN42} - A_{1s}V_{sN12} - A_{2s}V_{sN11} - A'_{1s}V_{N32} - A'_{2s}V_{N31},$$

$$V_{sN11} = V_{sA11}Z_{11} - V_{sA12}Z_{12} + \frac{h\psi_0\mu\nu^* h_{21}}{2a^3G(h_{21}^2 + h_{22}^2)} \frac{(I_{s01} - I_{s101})h_{11} + h_{12}(I_{s02} - I_{s102})}{h_{11}^2 + h_{12}^2}$$
$$+ \frac{h\psi_0\mu\nu^* h_{22}}{2a^3G(h_{21}^2 + h_{22}^2)} \frac{-(I_{s01} - I_{s101})h_{12} + h_{11}(I_{s02} - I_{s102})}{h_{11}^2 + h_{12}^2},$$

$$V_{sN12} = V_{sA11}Z_{12} + V_{sA12}Z_{11} - \frac{h\psi_0\mu\nu^* h_{22}}{2a^3G(h_{21}^2 + h_{22}^2)} \frac{(I_{s01} - I_{s101})h_{11} + h_{12}(I_{s02} - I_{s102})}{h_{11}^2 + h_{12}^2}$$
$$+ \frac{\psi_0 h\mu\nu^* h_{21}}{2a^3G(h_{21}^2 + h_{22}^2)} \frac{-(I_{s01} - I_{s101})h_{12} + h_{11}(I_{s02} - I_{s102})}{h_{11}^2 + h_{12}^2},$$

$$V_{sN21} = V_{sB11}Z_{11} - V_{sB12}Z_{12} + \frac{h\psi_0\mu\nu^* h_{21}}{2a^3G(h_{21}^2 + h_{22}^2)} \frac{(K_{s01} - K_{s101})h_{11} + h_{12}(K_{s02} - K_{s102})}{h_{11}^2 + h_{12}^2}$$
$$+ \frac{\psi_0 h\mu\nu^* h_{22}}{2a^3G(h_{21}^2 + h_{22}^2)} \frac{-(K_{s01} - K_{s101})h_{12} + h_{11}(K_{s02} - K_{s102})}{h_{11}^2 + h_{12}^2},$$

$$V_{sN22} = V_{sB11}Z_{12} + V_{sB12}Z_{11} - \frac{h\psi_0\mu\nu^* h_{22}}{2a^3G(h_{21}^2 + h_{22}^2)} \frac{(K_{s01} - K_{s101})h_{11} + h_{12}(K_{s02} - K_{s102})}{h_{11}^2 + h_{12}^2}$$
$$+ \frac{\psi_0 h\mu\nu^* h_{21}}{2a^3G(h_{21}^2 + h_{22}^2)} \frac{-(K_{s01} - K_{s101})h_{12} + h_{11}(K_{s02} - K_{s102})}{h_{11}^2 + h_{12}^2},$$

$$V_{sA21} = I_{s101} - H_{z21}\frac{(I_{s111}h_{11} + I_{s112}h_{12})}{h_{12}^2 + h_{11}^2} + H_{z22}\frac{-I_{s111}h_{12} + I_{s112}h_{11}}{h_{12}^2 + h_{11}^2},$$

$$V_{sA22} = I_{s102} - H_{z22}\frac{(I_{s111}h_{11} + I_{s112}h_{12})}{h_{12}^2 + h_{11}^2} - H_{z21}\frac{-I_{s111}h_{12} + I_{s112}h_{11}}{h_{12}^2 + h_{11}^2},$$

$$V_{sB21} = K_{s101} - H_{z21}\frac{K_{s111}h_{11} + K_{s112}h_{12}}{h_{12}^2 + h_{11}^2} + H_{z22}\frac{-K_{s111}h_{12} + K_{s112}h_{11}}{h_{12}^2 + h_{11}^2},$$

$$V_{sB22} = K_{s102} - H_{z22}\frac{K_{s111}h_{11} + K_{s112}h_{12}}{h_{12}^2 + h_{11}^2} - H_{z21}\frac{-K_{s111}h_{12} + K_{s112}h_{11}}{h_{12}^2 + h_{11}^2},$$

$$V_{sA11} = I_{s01} - H_{z11}\frac{I_{s11}h_{11} + I_{s12}h_{12}}{h_{12}^2 + h_{11}^2} + H_{z12}\frac{-I_{s11}h_{12} + I_{s12}h_{11}}{h_{12}^2 + h_{11}^2},$$

$$V_{sA12} = I_{s02} - H_{z12}\frac{I_{s11}h_{11} + I_{s12}h_{12}}{h_{12}^2 + h_{11}^2} - H_{z11}\frac{-I_{s11}h_{12} + I_{s12}h_{11}}{h_{12}^2 + h_{11}^2},$$

$$V_{sB11} = K_{s01} + H_{z11}\frac{K_{s11}h_{11} + K_{s12}h_{12}}{h_{12}^2 + h_{11}^2} + H_{z12}\frac{-K_{s11}h_{12} + K_{s12}h_{11}}{h_{12}^2 + h_{11}^2},$$

$$V_{sB12} = K_{s02} - H_{z12}\frac{K_{s11}h_{11} + K_{s12}h_{12}}{h_{12}^2 + h_{11}^2} - H_{z11}\frac{-K_{s11}h_{12} + K_{s12}h_{11}}{h_{12}^2 + h_{11}^2},$$

$$I_{s01} = 1 + \frac{b_2^2\cos 2\theta_1}{2^2} + \frac{b_2^4\cos 4\theta_1}{2^6} + \frac{b_4^6\cos 6\theta_1}{2^83} + \cdots,$$

$$I_{s02} = 1 + \frac{b_2^2\sin 2\theta_1}{2^2} + \frac{b_2^4\sin 4\theta_1}{2^6} + \frac{b_4^6\sin 6\theta_1}{2^83} + \cdots,$$

$$I_{sr01} = 1 + \frac{b_4^2\cos 2\theta_1}{2^2} + \frac{b_4^4\cos 4\theta_1}{2^6} + \frac{b_4^6\cos 6\theta_1}{2^83} + \cdots,$$

$$I_{sr02} = 1 + \frac{b_4^2 \sin 2\theta_1}{2^2} + \frac{b_4^4 \sin 4\theta_1}{2^6} + \frac{b_4^6 \sin 6\theta_1}{2^8 3} + \cdots,$$

$$I_{s11} = \frac{b_3}{2}\left\{\cos\theta_1\left(1 + \frac{b_3^2 \cos 2\theta_1}{2^3} + \frac{b_3^4 \cos 6\theta_1}{2^{10}3^2} + \cdots\right) - \sin\theta_1\left(\frac{b_3^2 \sin 2\theta_1}{2^3} + \frac{b_3^4 \sin 4\theta_1}{2^6 3} + \frac{b_3^6 \sin 6\theta_1}{2^{10}3^2} + \cdots\right)\right\},$$

$$I_{s12} = \frac{b_3}{2}\left\{\sin\dot{\theta}_1\left(1 + \frac{b_3^2 \cos 2\theta_1}{2^3} + \frac{b_3^4 \cos 6\theta_1}{2^{10}3^2} + \cdots\right) - \cos\theta_1\left(\frac{b_3^2 \sin 2\theta_1}{2^3} + \frac{b_3^4 \sin 4\theta_1}{2^6 3} + \frac{b_3^6 \sin 6\theta_1}{2^{10}3^2} + \cdots\right)\right\},$$

$$I_{sr11} = \frac{b_4}{3}\left\{\cos\theta_1\left(1 + \frac{b_4^2 \cos 2\theta_1}{2^3} + \frac{b_4^4 \cos 6\theta_1}{2^{10}3^2} + \cdots\right) - \sin\theta_1\left(\frac{b_4^2 \sin 2\theta_1}{2^3} + \frac{b_4^4 \sin 4\theta_1}{2^6 3} + \frac{b_4^6 \sin 6\theta_1}{2^{10}3^2} + \cdots\right)\right\},$$

$$I_{sr12} = \frac{b_4}{2}\left\{\sin\theta_1\left(1 + \frac{b_4^2 \cos 2\theta_1}{2^3} + \frac{b_4^4 \cos 6\theta_1}{2^{10}3^2} + \cdots\right) - \cos\theta_1\left(\frac{b_4^2 \sin 2\theta_1}{2^3} + \frac{b_4^4 \sin 4\theta_1}{2^6 3} + \frac{b_4^6 \sin 6\theta_1}{2^{10}3^2} + \cdots\right)\right\},$$

$$I_{s101} = 1 + \frac{b_3^2 \cos 2\theta_1}{2^2} + \frac{b_3^4 \cos 4\theta_1}{2^6} + \frac{b_3^6 \cos 6\theta_1}{2^8 3} + \cdots,$$

$$I_{s102} = 1 + \frac{b_3^2 \sin 2\theta_1}{2^2} + \frac{b_3^4 \sin 4\theta_1}{2^6} + \frac{b_3^6 \sin 6\theta_1}{2^8 3} + \cdots,$$

$$I_{s111} = \frac{b_3}{2}\left\{\cos\theta_1\left(1 + \frac{b_3^2 \cos 2\theta_1}{2^3} + \frac{b_3^4 \cos 6\theta_1}{2^{10}3^2} + \cdots\right) - \sin\theta_1\left(\frac{b_3^2 \sin 2\theta_1}{2^3} + \frac{b_3^4 \sin 4\theta_1}{2^6 3} + \frac{b_3^6 \sin 6\theta_1}{2^{10}3^2} + \cdots\right)\right\},$$

$$I_{s112} = \frac{b_3}{2}\left\{\sin\theta_1\left(1 + \frac{b_3^2 \cos 2\theta_1}{2^3} + \frac{b_3^4 \cos 6\theta_1}{2^{10}3^2} + \cdots\right) - \cos\theta_1\left(\frac{b_3^2 \sin 2\theta_1}{2^3} + \frac{b_3^4 \sin 4\theta_1}{2^6 3} + \frac{b_3^6 \sin 6\theta_1}{2^{10}3^2} + \cdots\right)\right\},$$

$$K_{s01} = -\ln\left(\frac{b_2}{2} + \gamma_1\right) I_{s01} + I_{s02}\tan^{-1}\frac{h_{12}}{h_{11}} + \left(\frac{b_2^2 \cos 2\theta_1}{2^2} + \left(1 + \frac{1}{2}\right)\frac{b_2^4 \cos 4\theta_1}{2^6} + \left(1 + \frac{1}{2} + \frac{1}{3}\right)\frac{b_2^6 \cos 6\theta_1}{2^6 3^2} + \cdots\right),$$

$$K_{s02} = -\ln\left(\frac{b_2}{2} + \gamma_1\right) I_{s02} - I_{s01}\tan^{-1}\frac{h_{12}}{h_{11}} + \left(\frac{b_2^2 \sin 2\theta_1}{2^2} + \left(1 + \frac{1}{2}\right)\frac{b_2^4 \sin 4\theta_1}{2^6} + \left(1 + \frac{1}{2} + \frac{1}{3}\right)\frac{b_2^6 \sin 6\theta_1}{2^{10}3^2} + \cdots\right),$$

$$K_{sr01} = -\ln\left(\frac{b_4}{2} + \gamma_1\right) I_{sr01} + I_{sr02}\tan^{-1}\frac{h_{12}}{h_{11}} + \left(\frac{b_4^2 \cos 2\theta_1}{2^2} + \left(1 + \frac{1}{2}\right)\frac{b_4^4 \cos 4\theta_1}{2^6} + \left(1 + \frac{1}{2} + \frac{1}{3}\right)\frac{b_4^6 \cos 6\theta_1}{2^6 3^2} + \cdots\right),$$

$$K_{sr02} = -\ln\left(\frac{b_4}{2} + \gamma_1\right) I_{sr02} - I_{sr01}\tan^{-1}\frac{h_{12}}{h_{11}}$$

$$+\left(\frac{b_4^2\sin 2\theta_1}{2^2}+\left(1+\frac{1}{2}\right)\frac{b_4^4\sin 4\theta_1}{2^6}+\left(1+\frac{1}{2}+\frac{1}{3}\right)\frac{b_4^6\sin 6\theta_1}{2^{10}3^2}+\cdots\right),$$

$$K_{s101}=-\ln\left(\frac{b_3}{2}+\gamma_1\right)I_{s01}+I_{s02}\tan^{-1}\frac{h_{12}}{h_{11}}$$
$$+\left(\frac{b_3^2\cos 2\theta_1}{2^2}+\left(1+\frac{1}{2}\right)\frac{b_3^4\cos 4\theta_1}{2^6}+\left(1+\frac{1}{2}+\frac{1}{3}\right)\frac{b_3^6\cos 6\theta_1}{2^6 3^2}+\cdots\right),$$

$$K_{s102}=-\ln\left(\frac{b_3}{2}+\gamma_1\right)I_{s02}-I_{s01}\tan^{-1}\frac{h_{12}}{h_{11}}$$
$$+\left(\frac{b_3^2\sin 2\theta_1}{2^2}+\left(1+\frac{1}{2}\right)\frac{b_3^4\sin 4\theta_1}{2^6}+\left(1+\frac{1}{2}+\frac{1}{3}\right)\frac{b_3^6\sin 6\theta_1}{2^{10}3^2}+\cdots\right),$$

$$K_{s11}=I_{s11}\ln\left(\frac{b_2}{2}+\gamma_1\right)-I_{s12}\tan^{-1}\frac{h_{32}}{h_{31}}+\frac{\cos\theta_1}{b_2}-\frac{1}{2}\left(b_2\cos\theta_1+\left[2+\frac{1}{2}\right]\frac{b_2^3\cos 3\theta_1}{2^4}\right.$$
$$\left.+\left[2\left(1+\frac{1}{2}\right)+\frac{1}{3}\right]\frac{b_2^5\cos 5\theta_1}{2^7 3}+\left[2\left(1+\frac{1}{2}+\frac{1}{3}\right)+\frac{1}{4}\right]\frac{b_2^7\cos 7\theta_1}{2^1 13^2}+\cdots\right),$$

$$K_{s12}=I_{s12}\ln\left(\frac{b_2}{2}+\gamma_1\right)-I_{s11}\tan^{-1}\frac{h_{32}}{h_{31}}-\frac{\sin\theta_1}{b_2}-\frac{1}{2}\left(b_2\sin\theta_1+\left[2+\frac{1}{2}\right]\frac{b_2^3\sin 3\theta_1}{2^4}\right.$$
$$\left.+\left[2\left(1+\frac{1}{2}\right)+\frac{1}{3}\right]\frac{b_2^5\sin 5\theta_1}{2^7 3}+\left[2\left(1+\frac{1}{2}+\frac{1}{3}\right)+\frac{1}{4}\right]\frac{b_2^7\sin 7\theta_1}{2^1 13^2}+\cdots\right),$$

$$K_{s111}=I_{s11}\ln\left(\frac{b_3}{2}+\gamma_1\right)-I_{s12}\tan^{-1}\frac{h_{32}}{h_{31}}+\frac{\cos\theta_1}{b_3}-\frac{1}{2}\left(b_2\cos\theta_1+\left[2+\frac{1}{2}\right]\frac{b_3^3\cos 3\theta_1}{2^4}\right.$$
$$\left.+\left[2\left(1+\frac{1}{2}\right)+\frac{1}{3}\right]\frac{b_3^5\cos 5\theta_1}{2^7 3}+\left[2\left(1+\frac{1}{2}+\frac{1}{3}\right)+\frac{1}{4}\right]\frac{b_3^7\cos 7\theta_1}{2^1 13^2}+\cdots\right),$$

$$K_{s112}=I_{s12}\ln\left(\frac{b_3}{2}+\gamma_1\right)+I_{s11}\tan^{-1}\frac{h_{32}}{h_{31}}-\frac{\sin\theta_1}{b_3}-\frac{1}{2}\left(b_3\sin\theta_1+\left[2+\frac{1}{2}\right]\frac{b_3^3\sin 3\theta_1}{2^4}\right.$$
$$\left.+\left[2\left(1+\frac{1}{2}\right)+\frac{1}{3}\right]\frac{b_3^5\sin 5\theta_1}{2^7 3}+\left[2\left(1+\frac{1}{2}+\frac{1}{3}\right)+\frac{1}{4}\right]\frac{b_3^7\sin 7\theta_1}{2^1 13^2}+\cdots\right),$$

$$K_{sr11}=I_{sr11}\ln\left(\frac{b_4}{2}+\gamma_1\right)-I_{sr12}\tan^{-1}\frac{h_{32}}{h_{31}}+\frac{\cos\theta_1}{b_4}-\frac{1}{2}\left(b_4\cos\theta_1+\left[2+\frac{1}{2}\right]\frac{b_4^3\cos 3\theta_1}{2^4}\right.$$
$$\left.+\left[2\left(1+\frac{1}{2}\right)+\frac{1}{3}\right]\frac{b_4^5\cos 5\theta_1}{2^7 3}+\left[2\left(1+\frac{1}{2}+\frac{1}{3}\right)+\frac{1}{4}\right]\frac{b_4^7\cos 7\theta_1}{2^1 13^2}+\cdots\right),$$

$$K_{sr12}=I_{sr12}\ln\left(\frac{b_4}{2}+\gamma_1\right)+I_{sr11}\tan^{-1}\frac{h_{32}}{h_{31}}-\frac{\sin\theta_1}{b_4}-\frac{1}{2}\left(b_4\sin\theta_1+\left[2+\frac{1}{2}\right]\frac{b_4^3\sin 3\theta_1}{2^4}\right.$$
$$\left.+\left[2\left(1+\frac{1}{2}\right)+\frac{1}{3}\right]\frac{b_4^5\sin 5\theta_1}{2^7 3}+\left[2\left(1+\frac{1}{2}+\frac{1}{3}\right)+\frac{1}{4}\right]\frac{b_4^7\sin 7\theta_1}{2^1 13^2}+\cdots\right),$$

γ_1 being an Euler's constant.

REFERENCES

1. C.R. Cox, Wave propagation through Newtonian fluid contained within the thickwalled viscoelastic tube: The influence of wall compressibility, *J. Biomechanics* **3**, 317–335, (1970).
2. J.C. Misra and S. Chakravarty, Study of compressibility in vascular rheology, *Rheologica Acta* **19**, 318–388, (1980).
3. J.C. Misra and S. Chakravarty, A free vibration analysis for the human cranial system, *J. Biomechanics* **15**, 635–645, (1982).
4. J.C. Misra and K. Roychoudhury, Non-linear stress field in blood vessels under the action of connective tissues, *Blood Vessels* **19**, 19–29, (1982).
5. J.C. Misra and S.I. Singh, A study on the nonlinear flow of blood through arteries, *Bull. Math. Bio.* **49**, 257–277, (1987).

6. J.C. Misra and B.K. Sahu, Propagation of pressure waves through large vessels: A mathematical model of blood visco-elasticity, *Mathl. Comput. Modelling* **12** (3), 333–349, (1989).
7. M. Mishra and J.C. Misra, An anisotropic strip weakened by an array of cracks, *Int. J. Engng. Sci.* **21**, 187–198, (1983).
8. J.C. Misra and B.K. Kar, Momentum integral method for studying characteristics of blood through a stenosed vessel, *Biorheology* **26**, 23–35, (1989).
9. J.C. Misra, M.K. Patra and S.C. Misra, A non-Newtonian fluid model for blood flow through arteries under stenotic conditions, *J. Biomechanics* **26**, 1129–1141, (1993).
10. J.C. Misra and M.K. Patra, Laminar boundary-layer flow of a Newtonian fluid through a curved pipe—Some applications to arterial flow dynamics, *Int. J. Engng. Sci.* **32**, 1997–2010, (1994).
11. J.C. Misra and S.K. Ghosh, A mathematical model for the study of blood flow through a channel with permeable walls, *Acta Mechanica* **122**, 137–153, (1997).
12. D.E. Kenyon, Transient filtration in a porous elastic cylinder, *J. Appl. Mech.* **98**, 594–598, (1976).
13. D.E. Kenyon, A mathematical model of water flow through aortic tissue, *Bull. Math. Biol.* **41**, 79–90, (1979).
14. G. Jayaraman, Water transport in the arterial wall—A theoretical study, *J. Biomechanics* **16**, 833–840, (1983).
15. C.R. Ethier, Flow through mixed fibrous porous materials, *AIChE. J.* **37**, 1227–1236, (1991).
16. M. Nakamura and T. Sawada, Numerical study on the flow of a non-Newtonian fluid through an axisymmetric stenosis, *J. Biomech. Engng.* **110**, 137–143, (1988).
17. H.A. Hogan and M. Henriksen, An evaluation of a micropolar model for blood flow through an idealized stenosis, *J. Biomechanics* **22**, 211–218, (1989).
18. C. Tu and M. Deville, Pulsatile flow of non-Newtonian fluid through arterial stenoses, *J. Biomechanics* **29**, 899–908, (1996).
19. T. Ariman, M.A. Truk and N.D. Sylvester, On steady and pulsatile flow of blood, *J. Appl. Mech.* **97**, 1–6, (1974).
20. A. Tozern and R. Skalak, Micropolar fluid as model for suspensions of rigid spheres, *Int. J. Engng. Sci.* **15**, 511–524, (1977).
21. D.M. Wang and J.M. Tarbell, Modelling interstitial flow in an artery wall allows estimation of wall shear stress on smooth muscle cells, *J. Biomech. Engng.* **117**, 358–363, (1995).
22. T. Ariman, A.S. Cakmak and L.R. Hill, Flow of micropolar fluids between two concentric cylinders, *Phys. Fluids* **10**, 2545–2550, (1967).
23. M. Abramowitz and S.I. Stegun, *Handbook of Mathematical Functions*, Dover, New York, (1972).
24. M.J. Manton, Low Reynolds number flow in slowly varying axisymmetric tubes, *J. Fluid Mech.* **55**, 451–459, (1978).